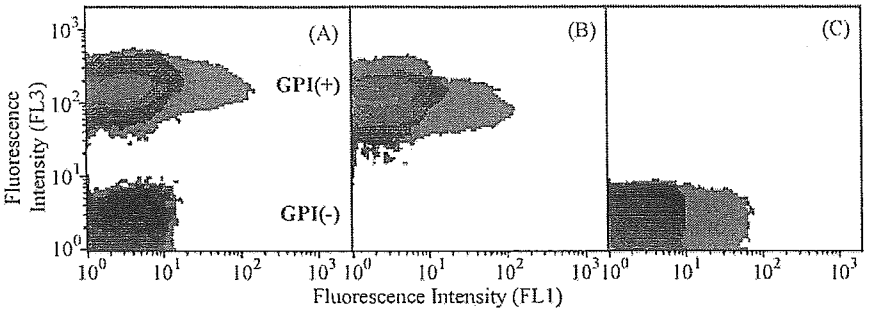

Fig. 2. *Py*RhopH complex binding to GPI-deficient erythrocytes. Representative density plot results of *Py*RhopH complex binding to GPI-deficient erythrocytes from a mouse harboring 28% GPI-deficient erythrocytes. Cell populations incubated with or without *P. yoelii* extracts are distinguished by red or blue coloring, respectively. No shift in FL1 fluorescence intensity was observed for the GPI-deficient erythrocyte population (A, lower), whereas the GPI-positive erythrocyte population shifted (A, upper). Erythrocytes from control mice stained with or without PE-Cy5 are shown as positive controls for *Py*RhopH complex binding for the upper (B) or lower (C) region. The density plot images were overlaid using Adobe Photoshop.

Table 3
The *Py*RhopH complex does not bind to GPI-deficient erythrocytes

Erythrocyte	Area	Status	INT_{exp}/INT_{ctl}[a]			
			Exp. #1[b]	Exp. #2	Exp. #3	Exp. #4
Chimeric Mouse	Upper	GPI (+)[c]	1.14, 1.14	1.33, 1.34	1.20, 1.36	1.18, 1.19[d]
	Lower	GPI (−)	0.96, 1.06	1.03, 1.04	0.97, 1.02	0.99, 1.01
Control Mouse	Upper	GPI (+)	1.21, 1.41	1.13, 1.26	1.21, 1.32	1.14, 1.19
	Lower	GPI (−)	1.18, 1.25	1.35, 1.36	1.19, 1.19	1.20, 1.21

[a] *Py*RhopH complex binding to the erythrocyte surface were given as a value obtained by dividing the geometric mean of fluorescence intensity of the experimental samples (with extract; INT_{exp}) by that of the control samples (without extract; INT_{ctl}).
[b] Experiments 1 and 2 were performed using a mouse with 28% GPI-deficient erythrocytes and experiments 3 and 4 using a mouse having 5% GPI-deficient erythrocytes. Data using mAb#25 were shown. Similar results were also obtained using mAb#32 (not shown).
[c] GPI (+) indicates GPI-positive and GPI (−) indicates GPI-deficient erythrocytes.
[d] Statistical differences ($P<.01$) are indicated between two groups using combined data from four experiments.

was not increased for the GPI-deficient population (Fig. 2A, lower). *Py*RhopH complex binding to control wild type erythrocytes were detected either with or without anti-CD24 mAb as shown in Fig. 2B and C. FL1 fluorescence intensity was not increased for negative control human erythrocytes (not shown). Experiments were done twice for each mouse and the results were summarized in Table 3. These data indicated that *Py*RhopH complex binding to GPI-deficient erythrocytes was reduced to an undetectable level using our flow cytometric binding assay.

3.6. GPI-deficient erythrocyte is resistant for P. yoelii invasion, but supports normal growth

To evaluate parasite invasion and growth in GPI-deficient erythrocytes, a mouse harboring 28% GPI-deficient erythrocytes was infected with *P. yoelii* 17X (lethal). When parasitemias reached 3.5% (smear #1) and 4.8% (smear #2), assayed by Giemsa stains of peripheral blood smears, the infection rates were independently evaluated for GPI-positive and GPI-deficient erythrocyte populations. Parasites iden-

Table 4
Invasion and development of *P. yoelii* parasites in GPI-deficient erythrocytes

Smear[a]	Status	Counted erythrocytes	Infected erythrocytes	Stage[b]		
				Early T	Late T	Schiz
#1	GPI (+)[c]	4534	159 (3.51%)[d,e]	107 (2.36%)	50 (1.10%)	2 (0.04%)
	GPI (−)	5962	100 (1.38%)	80 (1.34%)	17 (0.29%)	3 (0.04%)
#2	GPI (+)	3077	153 (4.97%)[e]	104 (3.38%)	45 (1.45%)	4 (0.13%)
	GPI (−)	3666	100 (2.73%)	66 (1.80%)	32 (0.87%)	2 (0.05%)

[a] Blood smears were made from an infected mouse when parasitemias reached 3.5% (smear #1) and 4.8% (smear #2).
[b] Representative images for each stage are shown in Fig. 3B. Early T, early trophozoite; Late T, late trophozoite; Schiz, schizont-stage parasites.
[c] GPI (+) indicates GPI-positive and GPI (−) indicates GPI-deficient erythrocytes.
[d] The infection rates are shown in the parenthesis.
[e] Infection rates of GPI-deficient erythrocytes are significantly lower than that of GPI-positive erythrocytes ($P<.01$).

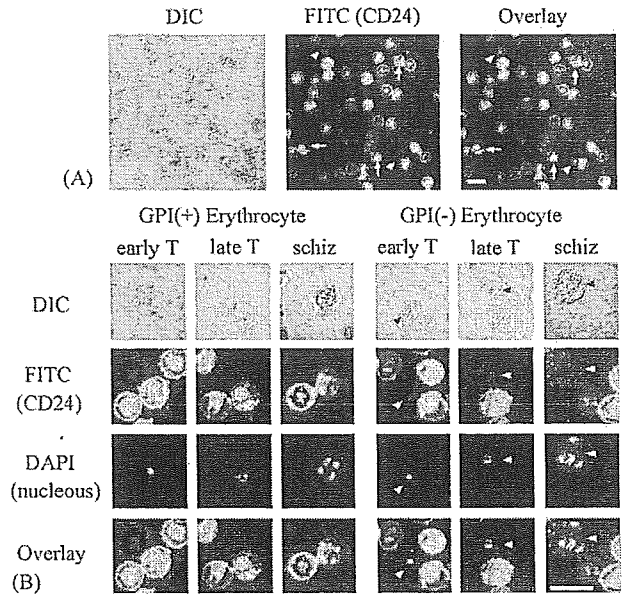

Fig. 3. *P. yoelii* infection of GPI-deficient erythrocytes. Thin blood smears were prepared from a mouse harboring 28% GPI-deficient erythrocytes 3 days after parasite inoculation. Air-dried thin blood smears were fixed with 1% formaldehyde in PBS and GPI-positive erythrocytes were visualized with anti-mouse CD24 antibody and FITC (green). Parasites were visualized with DAPI (blue). Parasites were found in both GPI-positive (arrow) and GPI-deficient (arrow head) erythrocytes (A). In both GPI-positive (arrow) and GPI-deficient (arrow head) erythrocytes, parasites can be matured up to the schizont-stage (B). Scale bar = 5 μm.

tified by DAPI nuclear staining were found in both GPI-positive (Fig. 3A, arrow) and GPI-deficient (Fig. 3A, arrow head) erythrocytes; however, the infection rate in GPI-deficient erythrocytes was only 40–55% that of GPI-positive erythrocytes ($P < .01$; Table 4). The proportion of the various asexual parasite stages were similar between the two erythrocyte populations, defined by the size and the number of nuclei (early trophozoite, late trophozoite, and schizont) as shown in Fig. 3B. This indicated that GPI-deficient erythrocytes were partially resistant to *P. yoelii* infection, whereas subsequent parasite maturation was not affected.

4. Discussion

In this report, we have characterized the binding specificity of the RhopH complex to erythrocytes using the rodent malaria parasite, *P. yoelii*. *Py*RhopH complex binding to erythrocytes was species-specific, observed with mouse but not rabbit or human erythrocytes. Binding is abolished following treatment of erythrocytes with trypsin or chymotrypsin, but not with neuraminidase, suggesting involvement of an erythrocyte non-sialylated protein receptor. Neither GPA nor the DARC, both known *P. falciparum* and *P. vivax* malaria parasite receptors, were found to be major *P. yoelii* RhopH complex receptors using knockout mice harboring targeted disruptions of these gene loci. However, we found undetectable *Py*RhopH complex binding and significant reduction of the *P. yoelii* infection of the GPI-deficient erythrocytes. These results indicate that the major erythrocyte receptor for *Py*RhopH complex is a protein, directly or indirectly, attached to the erythrocyte surface via GPI-anchor and that GPI-deficient erythrocytes are resistant to *P. yoelii* infection.

The *P. yoelii* RhopH complex retains erythrocyte-binding activity following a facile freeze-thaw extraction from parasite pellets. This activity forms the basis of a simple, reproducible flow cytometry assay allowing us to characterize the binding of RhopH complexes to control and specific protein-deficient erythrocytes surfaces. A single reaction requires only 1 μl of packed erythrocytes, containing approximately 1×10^7 erythrocytes, far less than the 50 μl of packed erythrocytes required by a classical erythrocyte binding assay using density centrifugation through silicon oil [21]. Furthermore, flow cytometry gating discriminates the major erythrocyte population and thereby minimizes pseudopositive results typically observed due to carry-over of contaminating parasite proteins in the silicon oil-based assay [22]. Using the flow cytometric method we show that binding to mouse erythrocytes increased in a dose-dependent manner, indicating that this method assays binding in a semi-quantitative fashion. Saturation of the binding was not observed using up to 100 μl extract, which was the maximum amount used in this assay (not shown). Attempts to purify intact *Py*RhopH complex having a binding ability have been unsuccessful in our hands. However, the lack of binding of control recombinant protein introduced into parasite extracts indicates *Py*RhopH binding to mouse erythrocytes is a specific interaction.

We propose two possible models for RhopH complex function, based on *Py*RhopH binding to the GPI-anchored receptor. First, the parasite may stimulate recruitment of cholesterol-rich lipid micromembrane domains around the erythrocyte surface entry point via synapse formation of GPI-anchored proteins with the RhopH complex. In accordance with this model, RhopH complex proteins were observed to be released onto the erythrocyte surface following merozoite contact with erythrocytes [11]. Second, because GPI-anchored proteins are recruited into the parasitophorous vacuole membrane during vacuole formation [1] and the RhopH complex is mainly released into the vacuole [11], it is conceivable that the RhopH complex functions in the parasitophorous vacuole by interacting with erythrocyte molecules that are recruited into the PVM. Recently a RhopH complex component was detected on the erythrocyte cytosol side of the PVM in *P. falciparum* [23]. Although the mechanisms of RhopH complex translocation from the parasite- to erythrocyte cytosol-aspect of the PVM are still unknown, the RhopH complex binding to the membrane component may be linked to this process.

We found that GPI-deficient mouse erythrocytes were partially resistant to *P. yoelii* infection. Because GPI-deficient erythrocytes appear to support normal growth of *P. yoelii*, once infected, the low infectivity of *P. yoelii* to the GPI-deficient erythrocytes indicates that impairment occurs early in the asexual blood stage cycle. Thus we propose that the in-

fection resistance is due to refractory invasion, probably due to impairment of the interaction between the parasite ligand and the erythrocyte receptor. It is formally possible that the GPI-deficient erythrocytes are refractory to invasion due to a decrease in their "deformability"; however, we feel that this explanation is unlikely, because *P. falciparum* parasites efficiently invade and grow normally within GPI-deficient erythrocytes obtained from paroxysmal nocturnal hemoglobinuria patients [24,25].

What is the difference in the invasion efficiency of *P. yoelii* and *P. falciparum* parasites to GPI-deficient erythrocytes? Although, it is plausible that the RhopH complex binding does not serve an essential biological role in invasion and solely mediates increased invasion efficiency, if the resistance of the *P. yoelii* infection to the GPI-deficient erythrocyte were due to abolished or reduced *Py*RhopH complex binding, then the normal infection of GPI-deficient erythrocytes by *P. falciparum* might be explained as follows. First, it might be proposed that the *Pf*RhopH complex receptor is not a GPI-anchored erythrocyte surface protein. Second, because RhopH1, one of the components of the RhopH complex, is encoded by a multigene family consisting of at least five paralogous members in *P. falciparum*, it is plausible that *Pf*RhopH1 determines receptor specificity and that multiple *Pf*RhopH1 recognize non-GPI-anchored proteins. From this point of view, *pyrhoph1ap*, a *pyrhoph1a* paralog encoding *Py*RhopH1, may explain partial but not complete resistance of the GPI-deficient erythrocytes to the *P. yoelii* infection. Such findings of multiple invasion pathways are well documented for the *Plasmodium dbl-ebp* gene family [26]. For example, *P. vivax* cannot invade erythrocytes lacking DARC, the receptor for the *P. vivax* Duffy binding protein (*Pv*DBP), a *P. vivax dbl-ebp* gene product. However, EBA-175, one of the *P. falciparum dbl-ebp* gene products, binds GPA, but *P. falciparum* can efficiently invade GPA-deficient erythrocytes. This might be explained by the paralogous gene products of EBA-175, such as BAEBL and JESEBL, which bind proteins other than GPA on the erythrocyte surface [27,28].

It is of interest to determine if erythrocyte GPI-anchored proteins are involved in human malaria parasite erythrocyte invasion, such as decay-accelerating factor (DAF, CD55; bearing Cromer blood group), Dombrock (Do) glycoprotein (Dombrock blood group) and acetylcholinesterase (Cartwright blood group). It should be also noted that GPI-anchored proteins may play important roles for the host cell invasion by other members of the apicomplexa such as *Toxoplasma gondii*, which is known to recruit GPI-anchored-proteins into the PVM [29].

Acknowledgements

We thank K. Kameda (INCS, Ehime University) for helping with the flow cytometry analysis. We also thank T.J. Templeton (Weill Medical College of Cornell University) for critical reading of the manuscript. Animal experiments in this study were carried out in compliance with the Guide for Animal Experimentation at Ehime University School of Medicine. This work was supported by grants from the Ministry of Education, Culture, Sports, Science and Technology, Japan (14370084 and 15406015 to M.T.; 15790215 to O.K.).

References

[1] Lauer S, VanWye J, Harrison T, et al. Vacuolar uptake of host components, and a role for cholesterol and sphingomyelin in malarial infection. EMBO J 2000;19:3556–64.
[2] Campbell GH, Miller LH, Hudson D, Franco EL, Andrysiak PM. Monoclonal antibody characterization of *Plasmodium falciparum* antigens. Am J Trop Med Hyg 1984;33:1051–4.
[3] Holder AA, Freeman RR, Uni S, Aikawa M. Isolation of a *Plasmodium falciparum* rhoptry protein. Mol Biochem Parasitol 1985;14:293–303.
[4] Lustigman S, Anders RF, Brown GV, Coppel RL. A component of an antigenic rhoptry complex of *Plasmodium falciparum* is modified after merozoite invasion. Mol Biochem Parasitol 1988;30:217–24.
[5] Hienne R, Ricard G, Fusaï T, et al. *Plasmodium yoelii*: Identification of rhoptry proteins using monoclonal antibodies. Exp Parasitol 1998;90:230–5.
[6] Brown HJ, Coppel RL. Primary structure of a *Plasmodium falciparum* rhoptry antigen. Mol Biochem Parasitol 1991;49:99–110.
[7] Shirano M, Tsuboi T, Kaneko O, Tachibana M, Adams JH, Torii M. Conserved regions of the *Plasmodium yoelii* rhoptry protein RhopH3 revealed by comparison with the *P. falciparum* homologue. Mol Biochem Parasitol 2001;112:297–9.
[8] Kaneko O, Tsuboi T, Ling IT, et al. The high molecular mass rhoptry protein, RhopH1, is encoded by members of the *clag* multigene family in *Plasmodium falciparum* and *Plasmodium yoelii*. Mol Biochem Parasitol 2001;118:237–45.
[9] Ling IT, Kaneko O, Narum DL, et al. Characterization of the *rhoph2* gene of *Plasmodium falciparum* and *Plasmodium yoelii*. Mol Biochem Parasitol 2003;127:47–57.
[10] Ling IT, Florens L, Dluzewski AR, et al. The *Plasmodium falciparum clag9* gene encodes a rhoptry protein that is transferred to the host erythrocyte upon invasion. Mol Microbiol 2004;52:107–18.
[11] Sam-Yellowe TY, Shio H, Perkins ME. Secretion of *Plasmodium falciparum* rhoptry protein into the plasma membrane of host erythrocytes. J Cell Biol 1988;106:1507–13.
[12] Sam-Yellowe TY, Perkins ME. Interaction of the 140/130/110 kDa rhoptry protein complex of *Plasmodium falciparum* with the erythrocyte membrane and the liposomes. Exp Parasitol 1991;73:161–71.
[13] Siddiqui WA, Tam LQ, Kramer KJ, et al. Merozoite surface coat precursor protein completely protects *Aotus* monkeys against *Plasmodium falciparum* malaria. Proc Natl Acad Sci USA 1987;84:3014–8.
[14] Cooper JA, Ingram LT, Bushell GR, et al. The 140/130/105 kilodalton protein complex in the rhoptries of *Plasmodium falciparum* consists of discrete polypeptides. Mol Biochem Parasitol 1988;29:251–60.
[15] Doury JC, Bonnefoy S, Roger N, Dubremetz JF, Mercereau-Puijalon O. Analysis of the high molecular weight rhoptry complex of *Plasmodium falciparum* using monoclonal antibodies. Parasitology 1994;108:269–80.
[16] Cowman AF, Baldi DL, Healer J, et al. Functional analysis of proteins involved in *Plasmodium falciparum* merozoite invasion of red blood cells. FEBS Lett 2000;476:84–8.
[17] Tsuboi T, Cao YM, Hitsumoto Y, Yanagi T, Kanbara H, Torii M. Two antigens on zygotes and ookinetes of *Plasmodium yoelii* and *Plasmodium berghei* that are distinct targets of transmission-blocking immunity. Infect Immun 1997;65:2260–4.

[18] Fukuma N, Akimitsu N, Hamamoto H, Kusuhara H, Sugiyama Y, Sekimizu K. A role of the Duffy antigen for the maintenance of plasma chemokine concentrations. Biochem Biophys Res Commun 2003;303:137–9.
[19] Arimitsu N, Akimitsu N, Kotani N, et al. Glycophorin A requirement for expression of O-linked antigens on the erythrocyte membrane. Genes Cells 2003;8:769–77.
[20] Murakami Y, Kinoshita T, Maeda Y, Nakano T, Kosaka H, Takeda J. Different roles of glycosylphosphatidylinositol in various hematopoietic cells as revealed by a mouse model of paroxysmal nocturnal hemoglobinuria. Blood 1999;94:2963–70.
[21] Klotz FW, Orlandi PA, Reuter G, et al. Binding of *Plasmodium falciparum* 175-kilodalton erythrocytes binding antigen and invasion of murine erythrocytes requires *N*-acetylneuraminic acid but not its O-acetylated form. Mol Biochem Parasitol 1992;51:49–54.
[22] Lobo CA, Rodriguez M, Reid M, Lustigman S. Glycophorin C is the receptor for the *Plasmodium falciparum* erythrocyte binding ligand PfEBP-2 (baebl). Blood 2003;101:4628–31.
[23] Hiller NL, Akompong T, Morrow JS, Holder AA, Haldar K. Identification of a stomatin orthologue in vacuoles induced in human erythrocytes by malaria parasites. A role for microbial raft proteins in apicomplexan vacuole biogenesis. J Biol Chem 2003;278: 48413–21.
[24] Soubes SC, Reid ME, Kaneko O, Miller LH. Search for the sialic acid-independent receptor on red blood cells for invasion by *Plasmodium falciparum*. Vox Sang 1999;76:107–14.
[25] Pattanapanyasat K, Walsh DS, Yongvanitchit K, Wattanasakul N, Wanachiwanawin W, Webster KH. Robust in vitro replication of *Plasmodium falciparum* in glycosyl-phosphatidylinositol-anchored membrane glycoprotein-deficient red blood cells. Am J Trop Med Hyg 2003;69:360–5.
[26] Adams JH, Kaneko O, Blair PL, Peterson DS. An expanding *ebl* family of *Plasmodium falciparum*. Trends Parasitol 2001;17:297–9.
[27] Mayer DC, Kaneko O, Hudson-Taylor DE, Reid ME, Miller LH. Characterization of a *Plasmodium falciparum* erythrocyte-binding protein paralogous to EBA-175. Proc Natl Acad Sci USA 2001;98:5222–7.
[28] Gilberger TW, Thompson JK, Triglia T, Good RT, Duraisingh MT, Cowman AF. A novel erythrocyte binding antigen-175 paralogue from *Plasmodium falciparum* defines a new trypsin-resistant receptor on human erythrocytes. J Biol Chem 2003;278:14480–6.
[29] Mordue DG, Desai N, Dustin M, Sibley LD. Invasion by *Toxoplasma gondii* establishes a moving junction that selectively excludes host cell plasma membrane proteins on the basis of their membrane anchoring. J Exp Med 1999;190:1783–92.

Available online at www.sciencedirect.com
SCIENCE DIRECT®
Molecular & Biochemical Parasitology 143 (2005) 20–28
MOLECULAR & BIOCHEMICAL PARASITOLOGY

Apical expression of three RhopH1/Clag proteins as components of the *Plasmodium falciparum* RhopH complex☆

Osamu Kaneko[a,*], Brian Y.S. Yim Lim[b], Hideyuki Iriko[a], Irene T. Ling[b], Hitoshi Otsuki[a], Munira Grainger[b], Takafumi Tsuboi[c], John H. Adams[d], Denise Mattei[e], Anthony A. Holder[b], Motomi Torii[a]

[a] *Department of Molecular Parasitology, Ehime University School of Medicine, Toon, Shigenobu-cho, Ehime 791-0295, Japan*
[b] *Division of Parasitology, MRC National Institute for Medical Research, The Ridgeway, Mill Hill, London NW7 1AA, UK*
[c] *Cell-Free Science and Technology Research Center, Ehime University, Matsuyama, Ehime 790-8577, Japan*
[d] *Department of Biological Sciences, University of Notre Dame, Notre Dame, Indiana 46556, USA*
[e] *Institut Pasteur, Biology of Host Parasite Interactions, URA 2581, F-75724, Paris CEDEX 15, France*

Received 25 January 2005; received in revised form 28 April 2005; accepted 2 May 2005
Available online 31 May 2005

Abstract

The *Plasmodium falciparum* high molecular mass rhoptry protein ('PfRhopH') complex is important for parasite growth and comprises three distinct gene products: RhopH1, RhopH2 and RhopH3. We have previously shown that *P. falciparum* RhopH1 is encoded by either PFC0110w (*clag3.2*) or PFC0120w (*clag3.1*), members of the previously-named *clag* (cytoadherence-linked asexual gene) multigene family. In this report, we have further characterized *rhoph1/clag* members in terms of gene structure, transcription and protein expression. The cDNA sequences for all five *rhoph1/clag* members were determined, confirming previous in silico predictions of intron–exon boundaries. All member genes were transcribed in HB3 and 3D7 parasite lines, but *clag3.2* was not transcribed in Dd2 parasites. The peak abundance of transcripts for all genes was observed during the late schizont stage. Antisera specific to Clag2 and Clag3.1 localized these proteins to the apical end of merozoites in segmented schizonts, and both proteins are found to be components of the PfRhopH complex. PfRhopH complex that was immunoprecipitated with *anti*-Clag9 antibody contained neither Clag2 nor Clag3.1, thereby suggesting that PfRhopH complexes contain only individual *rhoph1/clag* gene products. Since the PfRhopH complex binds the erythrocyte surface, and RhopH2 and RhopH3 are encoded by single copy genes, the RhopH1/Clag proteins may serve to confer some degree of specificity to the roles of the individual complexes.

Keywords: Clag; Cytoadherence; Invasion; Malaria; Merozoite; Rhoptry

1. Introduction

Plasmodium species are obligate intracellular parasites and entry into host erythrocytes is a prerequisite for the development of asexual stages. *Plasmodium* merozoites discharge the contents of their apical organelles (micronemes, rhoptries, dense granules) during the invasion process. The molecules contained within these organelles, including erythrocyte binding proteins, are considered important for erythrocyte invasion and have been studied as vaccine targets with the aim of inducing antibodies to block invasion. For example, passive immunization with monoclonal antibodies specific for a 235-kDa erythrocyte binding protein in the rhoptry [1], or active immunization with the protein [2], protects mice against blood stage challenge with *Plasmodium yoelii*. Other erythrocyte binding molecules within rhoptries are in a complex of high molecular mass proteins (the

Abbreviations: aa, amino acid(s); cDNA, complementary DNA; clag, cytoadherence-linked asexual gene; gDNA, genomic DNA; nt, nucleotide(s); PCR, polymerase chain reaction; PBS, phosphate buffered saline; SSU rRNA, small subunit ribosomal RNA

☆ *Note:* Nucleotide sequence data reported in this paper are available in the GenBank™, EMBL, and DDBJ databases under the accession numbers: AB193597–AB193601.

* Corresponding author. Tel.: +81 89 960 5286; fax: +81 89 960 5287.
E-mail address: okaneko@m.ehime-u.ac.jp (O. Kaneko).

0166-6851/$ – see front matter © 2005 Elsevier B.V. All rights reserved.
doi:10.1016/j.molbiopara.2005.05.003

RhopH complex) comprised of three distinct polypeptides: RhopH1, RhopH2 and RhopH3 that are encoded by unrelated genes [3–6]. Antibodies against the *P. falciparum* RhopH (PfRhopH) complex partially inhibit growth of *P. falciparum* in vitro and in vivo, consistent with its potential as a vaccine target [7–9]. The PfRhopH complex binds the erythrocyte and distributes into the erythrocyte and parasitophorous vacuolar membranes [10,11], and has been detected in ring-stage parasites [5,12,13], indicating an important role during the establishment of the parasitophorous vacuole. The importance of the complex has further been emphasized by the failure of attempts to disrupt the *pfrhoph3* gene locus, suggesting that the gene is necessary for parasite survival [14].

The genes encoding RhopH3 in *P. falciparum* and *P. yoelii* were identified some years ago [15,16]. Detailed molecular and functional analysis of other members of the RhopH complex was hindered until the recent identification of the genes encoding RhopH1 and RhopH2 in *P. falciparum* and *P. yoelii* [13,17]. Interestingly, we found by MALDI-ToF analysis that *P. falciparum* RhopH1 was encoded by either PFC0110w (*clag3.2*) or PFC0120w (*clag3.1*) [17]. These two genes are members of a family originally defined by a cytoadherence-linked asexual gene on chromosome 9 (*clag9*) [18,19]. Although the *clag9* gene product was originally proposed to mediate cytoadhesion between host endothelial cells and the surface of infected erythrocytes, we have shown by immunoelectron microscopy and immunochemical means that Clag9 is actually located within the rhoptry bodies in the (developing) merozoite, and is a component of the RhopH complex [20]. Based on this association, we renamed the '*clag*' multigene family '*rhoph1/clag*' [17]. This work raises the possibility that other *rhoph1/clag* gene products are also components of the PfRhopH complex. With the exception of Clag9, the gene structure (including intron–exon boundaries), transcription and protein expression profiles of other RhopH1/Clag members have yet to be fully characterized.

In this paper we address the unresolved issues of gene structure, transcription and translation and determine the phylogenetic relationship of all known *rhoph1/clag* gene products. In addition, using specific antisera we demonstrate the apical localization of Clag2 and Clag3.1, and determine their associations with the PfRhopH complex.

2. Materials and methods

2.1. Parasite lines

The 3D7, HB3, and Dd2 cloned lines of *P. falciparum* and 20 progeny between HB3 and Dd2, 1BB5, 3BA6, 3BD5, B1SD, B4R3, GC03, GC06, QC01, QC13, QC23, QC34, SC01, SC05, TC05, TC08, C188, C408, Ch3-116, Ch3-61, and D43 (kind gift from Dr. Wellems, NIH) [21] were maintained in vitro, essentially as previously described [22].

2.2. DNA and RNA isolation

Genomic DNA (gDNA) was isolated from *P. falciparum* using IsoQuick™ (Orca Research Inc., Bothell, WA). To obtain complementary DNA (cDNA), parasites at the schizont-stage were purified by differential centrifugation on a 70/40% Percoll-sorbitol gradient. To determine transcription throughout the asexual stages, parasites were synchronized using a MACS Type-D depletion column in conjunction with a SuperMACS II magnetic separator (Miltenyi Biotec GmbH, Germany) [13,23,24]. Schizonts were purified by passing a culture through the magnetized column, after which released merozoites were allowed to invade uninfected erythrocytes for 4 h before the removal of all remaining schizonts using the magnet. Part of the culture was harvested immediately and every 6 h thereafter. Total RNA was isolated from parasite-infected erythrocytes stored at −20 °C in RNA*later*™ (Qiagen, Valencia, CA), using the RNeasy Mini Kit (Qiagen). Following DNase treatment, cDNA was generated with random hexamers using an Omniscript Reverse Transcription Kit (Qiagen).

2.3. Identification of the chromosomal location of clagb1

Oligonucleotides were designed to differentiate between the *clagb1* genes of HB3 and Dd2 parasite lines. These were based on preliminary sequence data from the two lines (data not shown). Specific DNA fragments were PCR-amplified using 5′-GCTTATAATATAAAAATTCACGTTTTCG-3′ (common) and 5′-AAGTTCAACAAGTAATCATTTTAGTGG-3′ (specific for HB3) or 5′-ATAGGTAAAACAAGTACTTATATTAAATC-3′ (specific for Dd2). PCR amplification was performed for 20 progeny between HB3 and Dd2, and the inheritance pattern was compared with the segregation table [25].

2.4. Quantification of rhoph1/clag transcripts

Transcription of all five members of the *rhoph1/clag* family was evaluated in the HB3 parasite lines by real-time reverse transcription (RT)-PCR using the QuantiTect SYBR Green PCR Kit (Qiagen) and the LightCycler System (Roche). As a positive control, the gene for the asexual-type small subunit ribosomal RNA (A-Type SSU rRNA) was also evaluated. Oligonucleotides used are detailed in Table 1. The same oligonucleotides were used in the PCR amplification of 3D7 parasite line cDNA, generating DNA fragments, which were ligated into the pGEM-T Easy® plasmid (Promega, Madison, WI), and used in the production of a standard curve to evaluate the copy number of each transcript.

2.5. Recombinant protein expression

DNA fragments encoding N-terminal sequences specific to each of the RhopH1/Clag members were PCR-amplified

Table 1
Oligonucleotides used in the quantitative real-time RT-PCR of *pfrhoph1/clag* genes

Target gene	Oligonucleotide sequence
clag2	5′-TCATCACATAATTATTTCCTACATGAG-3′ 5′-TAATCTTGATATATATCTAAGGTTTTCAT-3′
clag3.1	5′-GGAGAAACACTTATATTAGGCGATAA-3′ 5′-TAATTTTTTAGTGCTAATTTTAATACGGT-3′
clag3.2	5′-GGAGAAACACTTATATTAGGCGATAA-3′ 5′-GTAATTTTTTAGTGCTAATTTTAATACAAC-3′
clag8	5′-CCCTTAGATAGTAATTTTATGAATGAAG-3′ 5′-TAATCTTGATAAATATCTAATGTTCTAAC-3′
clag9	5′-TAAAAGAAGTGGTAAATGATTTTTTTGTT-3′ 5′-CTTTCTCTCTATCTGCTTGGCTCAT-3′
SSU rRNA[a]	5′-ACGATCAGATACCGTCGTAATCTT-3′ 5′-CAATCTAAAAGTCACCTCGAAAGATG-3′

[a] Oligonucleotides previously detailed [26].

from *P. falciparum* HB3 gDNA and ligated into the pGEM-T Easy® plasmid. Inserts were digested with *Nhe*I and *Bam*HI, and ligated into the pJWE2 plasmid, yielding pCL2, pCL3.1, pCL3.2, pCL8, and pCL9 for DNA immunization [27,28]. Oligonucleotides used in the PCR amplification are detailed in Table 2. Recombinant proteins corresponding to the region used in the DNA immunization (Fig. 1) were produced in *E. coli* with the pET32b system (Novagen, Madison, WI) by ligating inserts into *Eco*RV site, yielding rCL2N, rCL3.1N, rCL3.2N, rCL8N, and rCL9N. Expressed recombinant proteins were detected using an *anti*-penta-His antibody (Qiagen) by Western blot analysis.

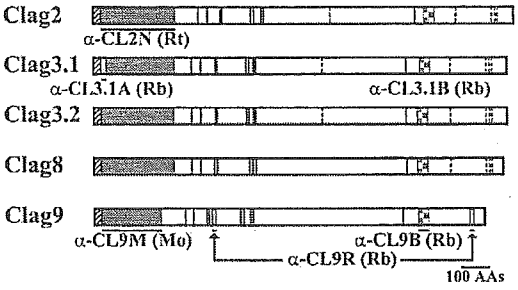

Fig. 1. Schematic illustrating the individual *Plasmodium falciparum* RhopH1/Clag family members showing the regions used in the generation of specific antisera. Shading indicates putative signal peptide sequences. Solid vertical lines indicate cysteine residues conserved throughout the multigene family, broken lines indicate those conserved in-part. Colored boxes illustrate regions used in the generation of specific sera: rabbit *anti*-Clag3.1 MAP-peptide serum A (α-CL3.1A) and rabbit *anti*-Clag9 peptides (α-CL9R) in solid green; rat *anti*-Clag2 DNA immunization serum (α-CL2N) and mouse *anti*-Clag9 DNA immunization serum (α-CL9M) in solid red; rabbit *anti*-Clag3.1 serum B (α-CL3.1B) and *anti*-Clag9 serum B (α-CL9B) in checkered red. Regions used only to check antibody specificity are in blue.

2.6. Production of RhopH1/Clag-specific antisera

DBA/2 mice and Wistar rats were immunized by intradermal injection in the ear pinna with 50 or 500 μg plasmid, four times at 3 week intervals, generating antisera α-CL2N, α-CL3.1N, α-CL3.2N, α-CL8N, and α-CL9N. Rabbit *anti*-CL3.1A serum was generated with MAP-peptide (NQNENDTISQNVNQH) corresponding to amino acid (aa) position 29–43 of Clag3.1. Rabbit *anti*-CL3.1B

Table 2
Oligonucleotides used in the production of PfRhopH1/Clag DNA immunization constructs and recombinant proteins

Protein (amino acid position)	Name	Oligonucleotide sequence[a]
Clag2 (25–271)	pCL2	5′-GCTAGCTCTATAAATGATAATGTAAATGAAAA-3′ 5′-CTCGAGGTGTGCATCCATTATTTCAATTT-3′
	rCL2N	5′-TTCTATAAATGATAATGTAAATGAAA-3′ 5′-TCGTGTGCATCCATTATTTCAA-3′
Clag3.1 (25–249)	pCL3.1	5′-GCTAGCTCAATAAATGAAAATCAAAATGAAAA-3′ 5′-CTCGAGATCGTTTGAATTCATTACATCTATTTTA-3′
	rCL3.1N	5′-TTCAATAAATGAAAATCAAAATGAAA-3′ 5′-TCGTTTGAATTCATTACATCTATT-3′
Clag3.2 (25–251)	pCL3.2	5′-GCTAGCTCAATAAATGAAAATGAAAATTTAGG-3′ 5′-CTCGAGGTTTGAATTCATTACATCTATTTTA-3′
	rCL3.2N	5′-TTCAATAAATGAAAATGAAAATTTAG-3′ 5′-TCGTTTGAATTCATTACATCTATT-3′
Clag8 (25–240)	pCL8	5′-GCTAGCTCCATTAATGAGAGTAAAAATGTGAATG-3′ 5′-CTCGAGATTTGTACTCATTAGATCTATTTTAGTAT-3′
	rCL8N	5′-TTCCATTAATGAGAGTAAAAATGT-3′ 5′-TCATTTGTACTCATTAGATCTATT-3′
Clag9 (24–222)	pCL9	5′-GCTAGCACCTACAAAGGAGATAATATAAAT-3′ 5′-CTCGAGATCATAATCAATTATATCAGATTTC-3′
	rCL9N	5′-TACCTACAAAGGAGATAATATAAA-3′ 5′-TCATCATAATCAATTATATCAGATT-3′

[a] *Nhe*I and *Bam*HI, restriction sites are underlined.

and *anti*-CL9B sera were generated by immunization with KLH-conjugated synthetic peptides (CSGYKSPESFFF and CKARTEGIIGKEWYK, respectively). Target regions used in the generation of the specific antisera are outlined in Fig. 1. The rabbit antiserum and mouse monoclonal antibody mAb 61.3 against PfRhopH2 and rabbit *anti*-Clag9 (α-CL9R) have been described previously [4,20]. Mouse *anti*-SERA5 (α-SE47′) was a kind gift from T. Horii at Osaka University [29].

2.7. SDS-PAGE and western blot analysis

SDS-extracted proteins from *P. falciparum* or recombinant proteins were dissolved in SDS-PAGE loading buffer, incubated at 100 °C for 3 min, and subjected to electrophoresis on a 5–20% polyacrylamide gel (ATTO, Japan). Proteins were then transferred to a 0.22 μm PVDF membrane (Bio-Rad, Hercules, CA). The proteins were immunostained with antisera followed by horseradish peroxidase-conjugated secondary antibody (Biosource Int., Camarillo, CA) and visualized with ECL Plus (Amersham Biosciences) on RX-U film (Fuji, Japan). The relative molecular sizes of the parasite-encoded proteins were calculated by reference to molecular size standards (BioRad).

2.8. Immunofluorescence microscopy

Thin smears of schizont-enriched *P. falciparum*-infected erythrocytes (Dd2) were prepared on glass slides and stored at −20 °C or −80 °C. The smears were thawed, acetone-fixed, and preincubated with PBS containing 5% non-fat milk at 37 °C for 30 min. They were then incubated with *anti*-RhopH1/Clag antisera at 37 °C for 1 h, followed by fluorescein isothiocyanate (FITC)-conjugated goat *anti*-(IgG and IgM) secondary antibody (Jackson ImmunoResearch Laboratories, West Grove, PA) and Alexa546-conjugated goat *anti*-(IgG and IgM) secondary antibody (Molecular Probes, Eugene, OR) at 37 °C for 30 min. High resolution image-capture and processing were performed using a fluorescence microscope (BX50; Olympus, Japan) and digital camera (IM500; Leica, Germany). 3D7 parasite samples were treated in a similar manner, with the exception of the blocking step, which was performed using PBS with 1% BSA. Clag3.1 and RhopH2 were visualized using rabbit *anti*-CL3.1B and mAb 61.3 followed by incubation with FITC-conjugated *anti*-rabbit IgG antibody (Sigma, Poole, UK) and Texas Red-conjugated *anti*-mouse IgG antibody (Sigma), respectively. Nuclei were stained with 4′,6-diamidino-2-phenylindole (DAPI) or Hoechst-33342 (Sigma). Slides were mounted in CitiFluor glycerol/PBS solution (CitiFluor Ltd, London, UK) and viewed under oil-immersion. Slides were examined using a DeltaVision cooled CCD Imaging System (Applied Precision LLC, Issaquah, WA). Images were analyzed using SoftWoRx, and processed in Adobe Photoshop (Adobe Systems Inc., San José, CA).

2.9. Phylogenetic analysis

To better understand the relationship amongst members of the *P. falciparum rhoph1/clag* multigene family, *Plasmodium vivax* homologs were WU-BLAST-searched (Gish, W. (1996–2004)) in the Institute for Genomic Research website (http://blast.wustl.edu) using amino acid sequences as a query. Deduced amino acid sequences of the first and last exons were used for phylogenetic analysis, since they are comparatively the largest (first exon 258–307 aa; last exon 427–494 aa). Unrooted trees were constructed using the CLUSTAL W algorithm and the Neighbor-Joining method using Kimura's Correction accompanied by Bootstrap Analysis with 1000 replicates [30–32]. The phylogenetic tree was constructed using TreeView [33].

3. Results

3.1. clagb1 is located on chromosome 8

We determined the chromosomal location of *clagb1* (also known as *clagBlob*, *clagb* or *clag7* due to initial assignments and preliminary annotations by the *P. falciparum* Genome Sequencing Project) by linkage analysis of 20 HB3 × Dd2 genetic-cross progeny [23], using nucleotide substitutions of *clagb*1 between HB3 and Dd2 lines as genotypic markers. The inheritance pattern was matched with the HRPII locus on the subtelomeric region of chromosome 8 (data not shown), hence we designate *clagb1* as *clag8* in this report.

3.2. RhopH1/Clag family members can be divided into two subgroups

The cDNA sequences of *clag2*, *-3.1*, and *-8* of Dd2 and *clag3.2* of HB3 were determined (accession numbers AB193597–AB193601) and the actual intron–exon boundaries confirmed the predictions by computer algorithm [17]. WU-BLAST search of the *P. vivax* database (The Institute for Genomic Research website at http://www.tigr.org) revealed three paralogous genes with accession numbers 1047, 3844, and 3944, respectively named as *pvrhoph1_1047*, *_3844*, and *_3944* in this report. Intron-exon boundaries were confirmed for the first and last introns of *pvrhoph1_1047* and *_3944* by sequencing RT-PCR products from *P. vivax* field isolates; the first and last exon sequences were used in the analysis. As the RT-PCR products for *pvrhoph1_3844* were not amplified, this gene was excluded from the analysis. The length of the deduced amino acid sequences of the first exons were 264 and 258 aa, and for the last exons 501 and 428 aa, for PvRhopH1_1047 and _3944, respectively. Using deduced amino acid sequences from five *P. falciparum* (3D7 line), two *P. yoelii* (17XL strain), and two *P. vivax* (SalI strain) homologs, the phylogenetic relationship amongst *Plasmodium* RhopH1/Clag family members was

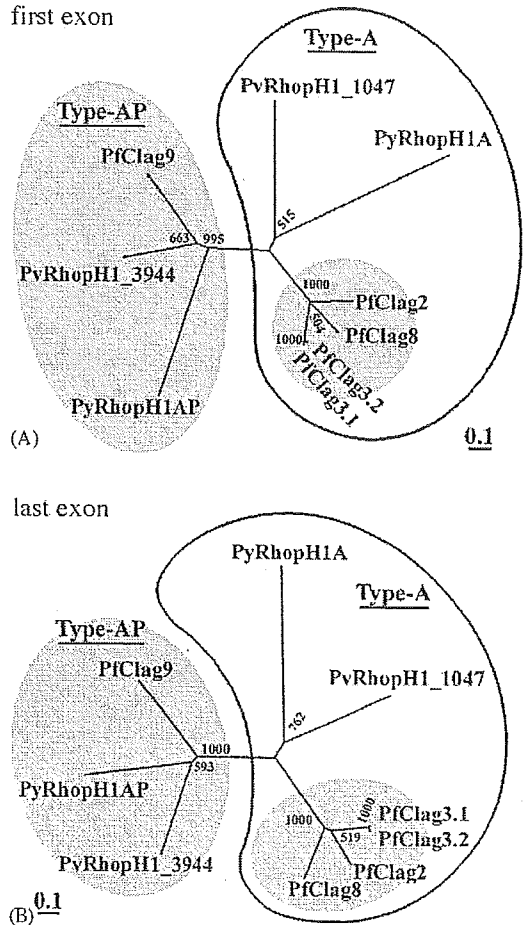

Fig. 2. Phylogenetic relationship between *Plasmodium* RhopH1/Clag proteins based on the deduced amino acid sequences of the first exon (Panel A) or last exon (Panel B) for *P. falciparum* (5 paralogs), *Plasmodium yoelii* (2 paralogs), and *Plasmodium vivax* (2 paralogs). Unrooted phylogenetic trees were constructed using the CLUSTAL W algorithm and the Neighbor-Joining method, using Kimura's Correction accompanied by Bootstrap Analysis with 1000 replicates. The number of amino acid substitutions per site of 0.1 is indicated. Groups differentiated from other proteins with the bootstrap values above 90% are masked. RhopH1/Clag family members were subdivided into two groups, Type-A and -AP, which are indicated on the tree.

analyzed (Fig. 2). Two unrooted phylogenetic trees imply the following. Clag9, PyRhopH1A-P, and PvRhopH1_3944 form a single group designated Type-AP, indicating that these three orthologs shared an ancestral gene, which had diversified from other RhopH1/Clag members before speciation in the *Plasmodium* genus occurred. RhopH1/Clag members can therefore be divided into two subgroups, Type-AP (as above) and Type-A that contains the remaining members. Additionally, the *P. falciparum* Type-A RhopH1/Clag group contains four paralogous members, implying the continued evolution of this subgroup. Preliminary analysis indicates that the remaining *P. vivax rhoph1* member, *pvrhoph1_3844*, belongs to the Type-A subgroup, also supporting the continued evolution of this subgroup (data not shown).

3.3. All five members of the pfrhoph1/clag multigene family are transcribed

RT-PCR amplifications using oligonucleotide sets specific for each *rhoph1/clag* family member in HB3, Dd2, and 3D7 parasite lines detected transcripts of all members, with the exception of *clag3.2* in Dd2 (data not shown). Thus, parasites have the ability to transcribe all five members.

To determine the transcription pattern through the asexual stages of the parasite life-cycle, quantitative RT-PCR was performed on the HB3 parasite line prepared from a synchronized culture harvested at 6 h intervals. Transcription was seen to peak for all members around 42–46 h after invasion, when parasites were in the schizont stage (Fig. 3). However, an earlier elevation in the number of *clag9* transcripts was observed at 36–40 h (6 h before the maximal peak), when the level of transcription of *clag9* was approximately 15% of its maximum, whilst that for other members was 0–5%. Transcriptome data compiled in the PlasmoDB web site [34,35] also indicated an earlier elevation of *clag9* transcripts compared with those of *clag2*, *-3.1*, and *-3.2*. Similar results showing a peak in transcription for all genes around 35–44 h post-invasion were observed in RT-PCR studies of *P. falciparum* 3D7 parasites prepared from a synchronized culture harvested at 3 h intervals (data not shown).

3.4. Production of antisera specific to Clag2, -3.1 and -9

Antisera were generated by DNA immunization using sequences selected from the N-terminal end of five RhopH1/Clag members and their specificity evaluated using *E. coli*-expressed recombinant protein. We found that the rat *anti*-Clag2 serum and mouse *anti*-Clag9 serum did not cross react with other members (Fig. 4A). Other antisera generated

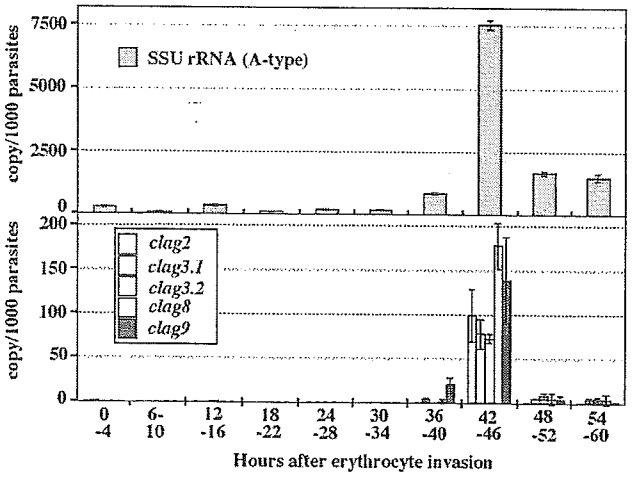

Fig. 3. Transcriptional analysis by quantitative RT-PCR of *rhoph1/clag* genes throughout the asexual blood stages of the *P. falciparum* (HB3 line) life-cycle. *Y*-axis indicates copy number of each transcript detected per 1000 parasites. Positive detection of the asexual-type small subunit ribosomal RNA (A-Type SSU rRNA) transcripts indicated successful cDNA synthesis. Error bars were generated from duplicates.

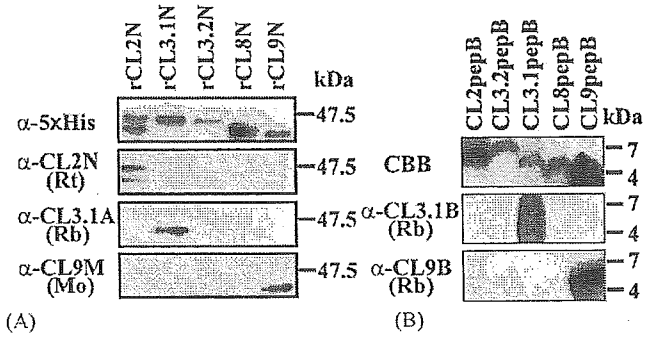

Fig. 4. Specificity of each antiserum against *E. coli*-expressed recombinant proteins for α-CL2N, α-CL3.1A, and α-CL9M (Panel A), and synthetic peptides for α-CL3.1B and α-CL9B (Panel B). CBB denotes Coomassie Brilliant Blue staining of synthetic peptides. The expressed regions of rCL2N, -3.1N, -3.2N, -8N, and -9N are indicated as filled boxes, CL2pepB, -3.1pepB, -3.2pepB, -8pepB, and -9pepB are indicated as checkered boxes in Fig. 1. α-5 × His indicates *anti*-penta His antibody.

in this manner showed cross-reactivity (data not shown), and were omitted from further analysis. The specificity of rabbit *anti*-Clag3.1 peptide serum A was confirmed using the same set of *E. coli*-expressed recombinant proteins (Fig. 4A) and that of rabbit *anti*-Clag3.1 peptide serum B and *anti*-Clag9 peptide serum B with synthetic peptides (Fig. 4B). Only antisera that were specific were used in the following studies.

3.5. Clag2 and -3.1 are expressed at the apical end of merozoites

All specific antisera against Clag members -2, -3.1, and -9 described above were used in indirect immunofluorescence assays (IFA), resulting in a specific reaction at the apical end of the merozoites in schizont-stage parasites. Overlaid images of the double-staining for *anti*-Clag3.1 and *anti*-PfRhopH2 or *anti*-Clag3.1 and *anti*-Clag9 sera reacting with segmented schizonts showed indistinguishable patterns of localization for these proteins (Fig. 5A–B). RhopH2 and Clag9 were previously shown to be located within the rhoptry body by immunoelectron microscopy [18], thus our IFA data suggest that Clag3.1 is localized within the rhoptries of segmented schizonts. Overlaid images of the double-staining for Clag2 and -3.1 also showed an indistinguishable pattern (Fig. 5C), indicating that Clag2 is also localized within the rhoptries of segmented schizonts. All segmented schizont-stage parasites observed by microscopy were positive for each RhopH1/Clag member, indicating that at least three members are co-expressed in all *P. falciparum* merozoites.

3.6. Clag2 and -3.1 are expressed in at least three parasite lines

Western blotting analysis was performed using the specific antisera shown to be reactive by IFA. To develop an appropriately effective extraction method for the RhopH

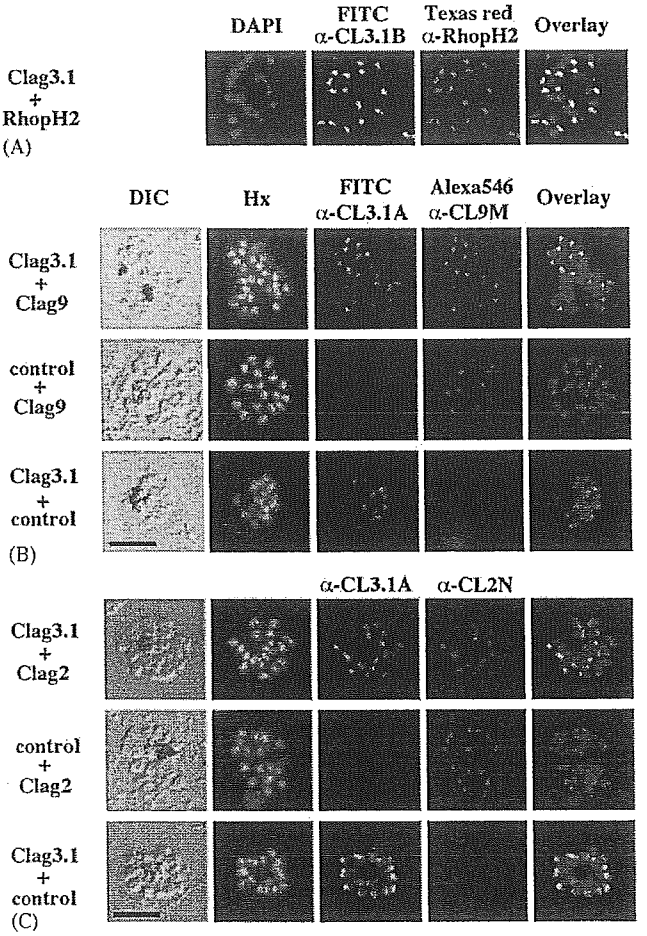

Fig. 5. Apical expression of RhopH1/Clag members -2, -3.1, and -9 in *P. falciparum* segmented schizonts. Schizont-infected erythrocytes were dual-labeled with α-CL3.1B and α-RhopH2 mAb 61.3 in the 3D7 parasite line (Panel A); α-CL3.1A and α-CL9M (Panel B) and α-CL3.1A and α-CL2N (Panel C) in Dd2 parasite line. Overlaid images are shown in the right-hand panels. All segmented schizont-stage parasites are positive for the antisera against Clag2, -3.1, and -9. Nuclei are counterstained with either DAPI or Hoechst-33342 (Hx). Scale bar represents 5 μm.

complex, parasite proteins were sequentially extracted from 3D7 schizont-stage parasites. Proteins were extracted by repeated freeze–thaw cycles in PBS, followed by extraction of the insoluble pellet in 1% Triton X-100. Finally, the Triton-insoluble fraction was dissolved in 2% SDS. The results indicated that most of Clag3.1 is extracted by a simple freeze–thaw step (Fig. 6A). Using the soluble freeze–thaw extract, we examined the protein expression of Clag2 and -3.1 in three parasite lines: 3D7, Dd2, and HB3. Antisera against Clag2 and Clag3.1 produced a specific reaction at approximately 155 kDa in Western Blot analysis of PBS soluble extracts from these three parasite lines (Fig. 6B).

3.7. Clag2 and -3.1 form a complex with RhopH2

We further examined if Clag2 and -3.1 were involved in the RhopH protein complex by Western blot analysis

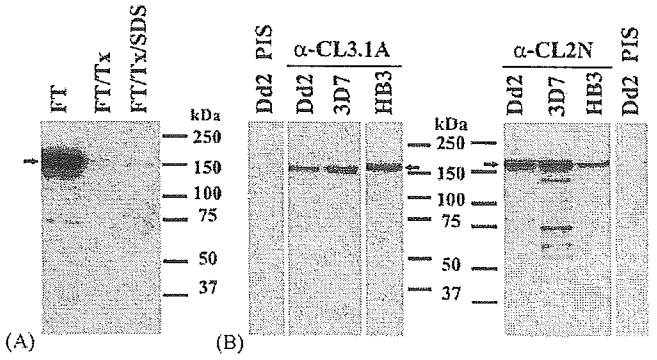

Fig. 6. Western blot analysis with *anti*-Clag2 (α-CL2N) and *anti*-Clag3.1 (α-CL3.1A) sera. (Panel A) Parasite proteins were sequentially extracted by repeated freeze–thaw cycles (FT) followed by 1% Triton X-100 (FT/Tx), then 2% SDS (FT/Tx/SDS) in PBS. Clag3.1 was exclusively detected in the sample extracted by simple freeze–thaw procedure. (Panel B) Clag2 and -3.1 were detected under reducing conditions as ~155 kDa bands in three parasite lines in the freeze–thaw fractions. 'PIS' denotes preimmune serum, which did not give any positive reactivity at 155 kDa when using Dd2 parasites.

of immunoprecipitated RhopH protein. Clag2, -3.1, and -9 were detected in the RhopH complex precipitated using *anti*-RhopH2 antiserum, indicating that these members are components of RhopH complex (Fig. 7). To examine if different RhopH1/Clag members co-exist in a single RhopH complex, the RhopH complex precipitated using *anti*-Clag9 serum was subjected to Western Blotting and the existence of other members of the RhopH1/Clag family was evaluated by probing with the specific antisera (Fig. 7). In this complex, RhopH2 and Clag9 were detected; however, Clag2 and -3.1 were not, indicating that Clag9 does not form a complex with these RhopH1/Clag members. *Anti*-SERA5 serum did not detect any signal in the *anti*-RhopH2 immunoprecipitate, thereby excluding any potential carryover due to insufficient or inadequate washing steps.

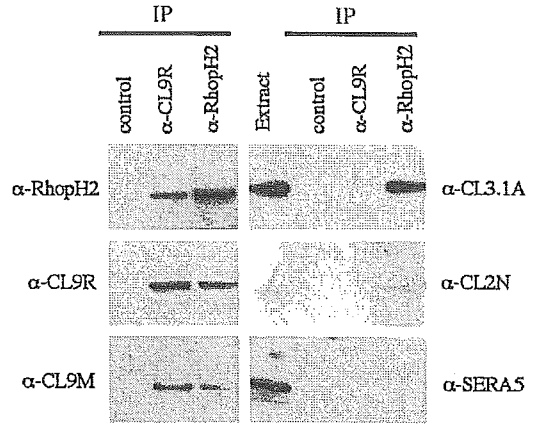

Fig. 7. Clag2, -3.1, and -9 are components of the RhopH complex, however, Clag2 and -3.1 do not form a complex with Clag9. Parasite extracts ('Extract') were immunoprecipitated ('IP') with rabbit *anti*-RhopH2 (α-RhopH2), *anti*-Clag9 (α-CL9R), or control normal sera and stained with rabbit *anti*-RhopH2, rabbit *anti*-Clag9 (α-CL9R), mouse *anti*-Clag9 (α-CL9M), rabbit *anti*-Clag3.1 (α-CL3.1A), rat *anti*-Clag2 (α-CL2N), or mouse *anti*-SERA5 sera.

4. Discussion

In this paper, we determined the cDNA sequences and transcription profiles of all five *rhoph1/clag* members throughout the asexual blood-stages of the *P. falciparum* life-cycle. Using a panel of specific antisera, the protein expression of Clag2 and -3.1 was demonstrated to be at the apical end of merozoites in segmented schizonts. Furthermore, these members were confirmed to be additional components of the RhopH complex, similar to Clag9 that we have previously shown to be apically expressed by IFA and localized to the rhoptry bodies by immunoelectron microscopy [20]. Clag2 and -3.1 appear not to be involved in RhopH complexes containing Clag9, suggesting that differing populations of RhopH complex exist, and each may contain only a single RhopH1/Clag member.

Initial releases of the *P. falciparum* genome sequence, and preliminary annotations contained numerous unassigned contigs, many of which were derived from "chromosome Blob"—a collective term representing chromosomes 6, 7, and 8, so-named due to the difficulty in separating these similarly-sized chromosomes. However, by linkage analysis we successfully located the gene locus for *clagb1* on the subtelomeric region of chromosome 8 and have consequently re-designated the gene '*clag8*' in accordance with its location. Once genomic DNA has been prepared from approximately 20 progeny of a *P. falciparum* genetic cross, linkage analysis is the most rapid and effective method of identifying a gene locus. The method employed in this report would assist the gap-closure process for further unassigned contigs.

Etzion et al. (1991) proposed that the PfRhopH complex would contain one each of RhopH1, RhopH2 and RhopH3, based on the estimated total molecular mass of the PfRhopH complex (approximately 480 kDa), which approximates to the sum of the individual molecular masses of RhopH1 (155 kDa), RhopH2 (140 kDa), and RhopH3 (110 kDa) [36]. This is consistent with our data showing that a RhopH complex containing Clag9 does not contain Clag2 or Clag3.1. Collectively, these data indicate that each RhopH complex contains only a single RhopH1/Clag member.

Phylogenetic analysis suggests that *rhoph1/clag* family members consist of two types, which were likely to have been created by a gene duplication event before speciation in the *Plasmodium* genus. Similar gene duplication events can be seen in other *Plasmodium* molecules, such as genes encoding ookinete surface proteins Pxs25 and Pxs28 or gametocyte surface proteins Pxs48 and Px47, which are tandemly located on the same chromosome, whereas Type-A and -AP of *rhoph1/clag* genes are located on separate chromosomes. This ancient branching between Type-A and -AP subgroups is potentially responsible for the different timing of the start of transcription between *clag9* and other members presented in Fig. 3, though the biological relevance still remains unclear.

Interestingly Type-A of the *rhoph1/clag* family was further duplicated in *P. falciparum* and *P. vivax*, but Type-AP

was not. One might speculate that the location on the chromosome generates this difference. For example, genes located on the subtelomeric region such as erythrocyte-binding-like (*ebl*), reticulocyte-binding-like (*rbl*), and *var* families are frequently multiplied. However, since *clag9* is also located in the subtelomeric region of the chromosome (similar to the other four *rhoph1/clag* members) this is unlikely to be the case. Another possibility is a selective advantage of the gene duplication of Type-A *rhoph1/clag* members due to an unknown function important to parasite survival. Other *Plasmodium* multigene family products involved in erythrocyte invasion increase the redundancy in recognition of the erythrocyte surface receptors, which is advantageous to parasite survival. For example, the *ebl* family was multiplied independently in *P. falciparum* and *P. knowlesi* and each member protein has different specificity to host erythrocyte receptors [37–41]. Because the RhopH complex has the ability to bind erythrocytes [11,42], and each RhopH complex is likely to contain only a single RhopH1/Clag member, it is plausible that RhopH1/Clag members function as a ligand domain of the RhopH complex and Type-A members are more important than Type-AP members. The reduced importance of the *clag9* gene is further supported by the observation that a panel of culture-adapted *P. falciparum* clones do not retain the *clag9* gene ([43], unpublished data). Whether the deletion of the *clag9* gene locus is an in vitro artifact or a commonly occurring natural event in the wild-type parasite population remains to be ascertained.

Malaria parasites utilize a number of transcriptional regulation mechanisms to escape host immunity. An example of this is the *P. yoelii rbl* family, *py235*. Transcripts of different *py235* members have been detected from individual merozoites in a single schizont [44]. We questioned whether this is also the case for the *rhoph1/clag* family members in *P. falciparum*. However, this appears to be unlikely since immunofluorescence microscopy with specific antisera indicates that all merozoites in a single schizont express at least three RhopH1/Clag members.

In summary, it is now evident that at least three RhopH1/Clag members are components of the RhopH complex, which suggests that the remaining two members (Clag3.2 and Clag8) are also RhopH complex components. Based on the molecular mass of the RhopH complex and the lack of Clag2 or Clag3.1 in the RhopH complex containing Clag9, we propose that each RhopH complex likely contains only a single RhopH1/Clag member, suggesting five different types of *P. falciparum* RhopH complex. It is therefore of interest to explore the binding specificity of each RhopH complex, as this would create further redundancy in erythrocyte invasion by *P. falciparum* merozoites.

Acknowledgements

We thank K. Okugawa and K. Oka in the Integrated Center for Science, Ehime University for their expertise, S. Takeji for sequencing and S. Ogun, NIMR, for her assistance with immunizations. We also thank J. Mullins for providing pJW4304 and T. Horii for the mouse *anti*-SERA5 serum. Preliminary sequence data for *P. vivax* was obtained from The Institute for Genomic Research website at http://www.tigr.org. Animal experiments in this study were carried out in compliance with the Guide for Animal Experimentation at Ehime University School of Medicine, and under certification of the UK Home Office Animals (Scientific Procedures) Act 1986. This work was supported in part by Grants-in-Aid for Scientific Research 14370084 and 15406015 (to M. T.) and Encouragement of Young Scientists 15790215 (to O.K.) from the Ministry of Education, Culture, Sports, Science and Technology, Japan. B.Y.S.Y.L. acknowledges the support of a Medical Research Council (UK) PhD Studentship.

References

[1] Freeman RR, Trejdosiewicz AJ, Cross GAM. Protective monoclonal antibodies recognizing stage-specific merozoite antigens of a rodent malaria parasite. Nature 1980;284:366–8.
[2] Holder AA, Freeman RR. Immunization against blood-stage rodent malaria using purified parasite antigens. Nature 1981;294:361–4.
[3] Campbell GH, Miller LH, Hudson D, Franco EL, Andrysiak PM. Monoclonal antibody characterization of *Plasmodium falciparum* antigens. Am J Trop Med Hyg 1984;33:1051–4.
[4] Holder AA, Freeman RR, Uni S, Aikawa M. Isolation of a *Plasmodium falciparum* rhoptry protein. Mol Biochem Parasitol 1985;14:293–303.
[5] Lustigman S, Anders RF, Brown GV, Coppel RL. A component of an antigenic rhoptry complex of *Plasmodium falciparum* is modified after merozoite invasion. Mol Biochem Parasitol 1988;30:217–24.
[6] Hienne R, Ricard G, Fusaï T, et al. *Plasmodium yoelii*: identification of rhoptry proteins using monoclonal antibodies. Exp Parasitol 1998;90:230–5.
[7] Siddiqui WA, Tam LQ, Kramer KJ, et al. Merozoite surface coat precursor protein completely protects *Aotus* monkeys against *Plasmodium falciparum* malaria. Proc Natl Acad Sci USA 1987;84:3014–8.
[8] Cooper JA, Ingram LT, Bushell GR, et al. The 140/130/105 kDa protein complex in the rhoptries of *Plasmodium falciparum* consists of discrete polypeptides. Mol Biochem Parasitol 1988;29:251–60.
[9] Doury JC, Bonnefoy S, Roger N, Dubremetz JF, Mercereau-Puijalon O. Analysis of the high molecular weight rhoptry complex of *Plasmodium falciparum* using monoclonal antibodies. Parasitology 1994;108:269–80.
[10] Sam-Yellowe TY, Shio H, Perkins ME. Secretion of *Plasmodium falciparum* rhoptry protein into the plasma membrane of host erythrocytes. J Cell Biol 1988;106:1507–13.
[11] Sam-Yellowe TY, Perkins ME. Interaction of the 140/130/110 kDa rhoptry protein complex of *Plasmodium falciparum* with the erythrocyte membrane and liposomes. Exp Parasitol 1991;73:161–71.
[12] Hiller NL, Akompong T, Morrow JS, Holder AA, Haldar K. Identification of a stomatin orthologue in vacuoles induced in human erythrocytes by malaria parasites. A role for microbial raft proteins in apicomplexan vacuole biogenesis. J Biol Chem 2003;278:48413–21.
[13] Ling IT, Kaneko O, Narum DL, et al. Characterisation of the *rhoph2* gene of *Plasmodium falciparum* and *Plasmodium yoelii*. Mol Biochem Parasitol 2003;127:47–57.
[14] Cowman AF, Baldi DL, Healer J, et al. Functional analysis of proteins involved in *Plasmodium falciparum* merozoite invasion of red blood cells. FEBS Lett 2000;476:84–8.

[15] Brown HJ, Coppel RL. Primary structure of a *Plasmodium falciparum* rhoptry antigen. Mol Biochem Parasitol 1991;49:99–110.
[16] Shirano M, Tsuboi T, Kaneko O, Tachibana M, Adams JH, Torii M. Conserved regions of the *Plasmodium yoelii* rhoptry protein RhopH3 revealed by comparison with the *P. falciparum* homologue. Mol Biochem Parasitol 2001;112:297–9.
[17] Kaneko O, Tsuboi T, Ling IT, et al. The high molecular mass rhoptry protein, RhopH1, is encoded by members of the *clag* multigene family in *Plasmodium falciparum* and *Plasmodium yoelii*. Mol Biochem Parasitol 2001;118:237–45.
[18] Holt DC, Gardiner DL, Thomas EA, et al. The cytoadherence linked asexual gene family of *Plasmodium falciparum*: are there roles other than cytoadherence? Int J Parasitol 1999;29:939–44.
[19] Trenholme KR, Gardiner DL, Holt D, et al. *clag9*: a cytoadherence gene in *P. falciparum* essential for binding parasitized erythrocytes to CD36. Proc Natl Acad Sci USA 2000;97:4029–33.
[20] Ling IT, Florens L, Dluzewski AR, et al. The *Plasmodium falciparum clag9* gene encodes a rhoptry protein that is transferred to the host erythrocyte upon invasion. Mol Microbiol 2004;52:107–18.
[21] Su X, Kirkman LA, Fujioka H, Wellems TE. Complex polymorphisms in an approximately 330 kDa protein are linked to chloroquine-resistant *P. falciparum* in Southeast Asia and Africa. Cell 1997;28(91):593–603.
[22] Trager W, Jensen JB. Human malaria parasites in continuous culture. Science 1976;193:673–5.
[23] Staalsoe T, Giha HA, Dodoo D, Theander TG, Hviid L. Detection of antibodies to variant antigens on *Plasmodium falciparum*-infected erythrocytes by flow cytometry. Cytometry 1999;35:329–36.
[24] Taylor HM, Grainger M, Holder AA. Variation in the expression of a *Plasmodium falciparum* protein family implicated in erythrocyte invasion. Infect Immun 2002;70:5779–89.
[25] Su X, Ferdig MT, Huang Y, et al. A genetic map and recombination parameters of the human malaria parasite *Plasmodium falciparum*. Science 1999;286:1351–3.
[26] Kimura M, Kaneko O, Liu Q, et al. Identification of the four species of human malaria parasites by nested PCR that targets various sequences in the small subunit rRNA gene. Parasitol Int 1997;46:91–5.
[27] Lu S, Arthos J, Montefiori DC, et al. Simian immunodeficiency virus DNA vaccine trial in macaques. J Virol 1996;70:3978–91.
[28] Kaneko O, Mu J, Tsuboi T, Su X, Torii M. Gene structure and expression of a *Plasmodium falciparum* 220-kDa protein homologous to the *Plasmodium vivax* reticulocyte binding proteins. Mol Biochem Parasitol 2002;121:275–8.
[29] Pang XL, Mitamura T, Horii T. Antibodies reactive with the N-terminal domain of *Plasmodium falciparum* serine repeat antigen inhibit cell proliferation by agglutinating merozoites and schizonts. Infect Immun 1999;67:1821–7.
[30] Thompson JD, Higgins DG, Gibson TJ. CLUSTAL W: improving the sensitivity of progressive multiple sequence alignment through sequence weighting, position-specific gap penalties and weight matrix choice. Nucleic Acids Res 1994;22:4673–80.
[31] Saitou N, Nei M. The neighbor-joining method: a new method for reconstructing phylogenetic trees. Mol Biol Evol 1987;4:406–25.
[32] Kimura M. A simple method for estimating evolutionary rate of base substitutions through comparative studies of nucleotide sequences. J Mol Evol 1980;16:111–20.
[33] Page RD. TreeView: an application to display phylogenetic trees on personal computers. Comput Appl Biosci 1996;12:357–8.
[34] Le Roch KG, Zhou Y, Blair PL, et al. Discovery of gene function by expression profiling of the malaria parasite life cycle. Science 2003;301:1503–8.
[35] PlasmoDB: An integrative database of the *Plasmodium falciparum* genome. Tools for accessing and analyzing finished and unfinished sequence data. Nucleic Acids Res 2001; 29:66–9.
[36] Etzion Z, Murray MC, Perkins ME. Isolation and characterization of rhoptries of *Plasmodium falciparum*. Mol Biochem Parasitol 1991;47:51–61.
[37] Adams JH, Hudson DE, Torii M, et al. The Duffy receptor family of *Plasmodium knowlesi* is located within the micronemes of invasive malaria merozoites. Cell 1990;63:141–53.
[38] Adams JH, Kaneko O, Blair PL, Peterson DS. An expanding *ebl* family of *Plasmodium falciparum*. Trends Parasitol 2001;17:297–9.
[39] Mayer DC, Kaneko O, Hudson-Taylor DE, Reid ME, Miller LH. Characterization of a *Plasmodium falciparum* erythrocyte-binding protein paralogous to EBA-175. Proc Natl Acad Sci USA 2001;98:5222–7.
[40] Gilberger TW, Thompson JK, Triglia T, et al. A novel erythrocyte binding antigen-175 paralogue from *Plasmodium falciparum* defines a new trypsin-resistant receptor on human erythrocytes. J Biol Chem 2003;278:14480–6.
[41] Mayer DC, Mu JB, Kaneko O, Duan J, Su XZ, Miller LH. Polymorphism in the *Plasmodium falciparum* erythrocyte-binding ligand JESEBL/EBA-181 alters its receptor specificity. Proc Natl Acad Sci USA 2004;101:2518–23.
[42] Rungruang T, Kaneko O, Murakami Y, et al. Erythrocyte surface glycosylphosphatidyl inositol anchored receptor for the malaria parasite. Mol Biochem Parasitol 2005;140:13–21.
[43] Day KP, Karamalis F, Thompson J, et al. Genes necessary for expression of a virulence determinant and for transmission of *Plasmodium falciparum* are located on a 0.3-megabase region of chromosome 9. Proc Natl Acad Sci USA 1993;90:8292–6.
[44] Preiser PR, Jarra W, Capiod T, Snounou G. A rhoptry-protein-associated mechanism of clonal phenotypic variation in rodent malaria. Nature 1999;398:618–22.

INFECTION AND IMMUNITY, Nov. 2005, p. 7375–7380 Vol. 73, No. 11
0019-9567/05/$08.00+0 doi:10.1128/IAI.73.11.7375–7380.2005

Nasal Immunization with a Malaria Transmission-Blocking Vaccine Candidate, Pfs25, Induces Complete Protective Immunity in Mice against Field Isolates of *Plasmodium falciparum*

Takeshi Arakawa,[1] Ai Komesu,[1] Hitoshi Otsuki,[2] Jetsumon Sattabongkot,[3] Rachanee Udomsangpetch,[4] Yasunobu Matsumoto,[5] Naotoshi Tsuji,[6] Yimin Wu,[7] Motomi Torii,[2] and Takafumi Tsuboi[8]*

Division of Molecular Microbiology, Center of Molecular Biosciences, University of the Ryukyus, Nishihara, Okinawa 903-0213, Japan[1]; Department of Molecular Parasitology, Ehime University School of Medicine, Toon, Ehime 791-0295, Japan[2]; Department of Entomology, Armed Forces Research Institute of Medical Sciences, Bangkok 10400, Thailand[3]; Department of Pathobiology, Faculty of Science, Mahidol University, Bangkok 10400, Thailand[4]; Laboratory of Global Animal Resource Science, Graduate School of Agricultural and Life Sciences, University of Tokyo, Yayoi, Bunkyo-ku, Tokyo 113-8657, Japan[5]; Laboratory of Parasitic Diseases, National Institute of Animal Health, National Agricultural Research Organization, Tsukuba, Ibaraki 305-0856, Japan[6]; Malaria Vaccine Development Branch, National Institute of Allergy and Infectious Diseases, National Institutes of Health, Rockville, Maryland 20852[7]; and Cell-Free Science and Technology Research Center, Ehime University, Matsuyama, Ehime 790-8577, Japan[8]

Received 28 June 2005/Returned for modification 25 July 2005/Accepted 20 August 2005

Malaria transmission-blocking vaccines based on antigens expressed in sexual stages of the parasites are considered one promising strategy for malaria control. To investigate the feasibility of developing noninvasive mucosal transmission-blocking vaccines against *Plasmodium falciparum*, intranasal immunization experiments with *Pichia pastoris*-expressed recombinant Pfs25 proteins were conducted. Mice intranasally immunized with the Pfs25 proteins in the presence of a potent mucosal adjuvant cholera toxin induced robust systemic as well as mucosal antibodies. All mouse immunoglobulin G (IgG) subclasses except IgG3 were found in serum at comparable levels, suggesting that the immunization induced mixed Th1 and Th2 responses. Consistent with the expression patterns of the Pfs25 proteins in the parasites, the induced immune sera specifically recognized ookinetes but not gametocytes. In addition, the immune sera recognized Pfs25 proteins with the native conformation but not the denatured forms, indicating that mucosal immunization induced biologically active antibodies capable of recognizing conformational epitopes of native Pfs25 proteins. Feeding *Anopheles dirus* mosquitoes with a mixture of the mouse immune sera and gametocytemic blood derived from patients infected with *P. falciparum* resulted in complete interference with oocyst development in mosquito midguts. The observed transmission-blocking activities were strongly correlated with specific serum antibody titers. Our results demonstrated for the first time that a *P. falciparum* transmission-blocking vaccine candidate is effective against field-isolated parasites and may justify the investigation of noninvasive mucosal vaccination regimens for control of malaria, a prototypical mucosa-unrelated mosquito-borne parasitic disease.

Malaria causes high mortality and morbidity in tropical and subtropical countries, killing more than 3 million people annually (4, 29). The emergence of drug-resistant parasites and insecticide-resistant mosquitoes has raised continued public health problems worldwide. Given their complex life cycle and the discrete nature of immune responses to each developmental stage, the malaria parasites provide many potential targets for the development of prophylactic vaccines. Transmission-blocking vaccines the target sexual stages of the parasites (i.e., gametocyte, gamete, zygote, and ookinete) (6). Transmission-blocking antibodies ingested together with the gametocytes block parasite development in the mosquito midgut, preventing parasite transmission to other susceptible individuals. Thus, transmission-blocking vaccines are expected to prevent the spread of escape mutants that could be emerging during the course of antimalaria drug treatment or other prophylactic vaccines targeting asexual stages of the parasites. A leading transmission-blocking vaccine candidate antigen against *Plasmodium falciparum* is the ookinete surface protein Pfs25 (17, 18), and a clinical-grade recombinant Pfs25 expressed in *Pichia pastoris* is now available (33).

Mucosal vaccination with nonreplicating particles or recombinant proteins in combination with effective mucosal adjuvants has demonstrated their ability to induce local protective immunity against mucosal pathogens (32). Nasal vaccines in particular are by far the most effective mucosal vaccines, capable of priming a full range of local as well as systemic immune responses against protective antigenic epitopes (13, 14). In addition, this type of topically administrable, needle-free, noninvasive vaccine may be safer than injection-based parenteral vaccines by reducing the risk of infection from blood-borne pathogens, and may also be cost-effective because ad-

* Corresponding author. Mailing address: Cell-free Science and Technology Research Center, Ehime University, 3 Bunkyo-cho, Matsuyama, Ehime 790-8577, Japan. Phone: 81-89-927-8277. Fax: 81-89-927-9941. E-mail: tsuboi@ccr.ehime-u.ac.jp.

ministration does not require highly trained medical or veterinary personnel.

Although mucosal vaccines have several attractive features over parenteral vaccines, their targets had been almost exclusively limited to mucosal infections, and their potential applicability to nonmucosal pathogens such as arthropod vector-borne parasites and viruses seemed to be unappreciated. However, previous studies with malaria parasites (1, 5, 15, 23, 24, 27, 30) and Japanese encephalitis virus (unpublished data), which are prototypical mosquito-borne infectious protozoa and virus, respectively, indicated that mucosal vaccines could be effective alternative immunization methods.

In this study we evaluated the ability of transmission-blocking mucosal vaccines against field isolates of *P. falciparum*. Our results indicate that recombinant Pfs25 is sufficiently immunogenic when coadministered intranasally with a mucosal adjuvant to achieve robust immune protection against parasite transmission, suggesting that noninvasive mucosal vaccines are a promising alternative approach for malaria prevention.

MATERIALS AND METHODS

Mice and immunization schedule. Six-week-old female BALB/c ($H\text{-}2^d$) and A/J ($H\text{-}2^a$) mice (Japan SLC, Hamamatsu, Japan) were used for intranasal immunization experiments. Groups of six to seven mice were intranasally immunized three times at weeks 0, 3, and 5 with 20 μg of *Pichia pastoris*-expressed recombinant Pfs25 (33) mixed with 1 μg of cholera toxin (CT; Sigma-Aldrich) as a mucosal adjuvant. The volume of the mixture was adjusted to 15 μl with phosphate-buffered saline (PBS) and administered to external nares with micropipette without anesthesia. As negative controls mice were intranasally administered with 1 μg of CT alone or PBS.

Serum and mucosal sample collection. Blood was collected from immunized mice one week after the third immunization by cardiac puncture under complete anesthesia confirmed by eyelid reflex responses. Immune sera prepared from the collected blood were used for antibody titer analysis and transmission-blocking assays. Nasal secretions were collected from exsanguinated animals immediately after sacrifice by washing the nasal cavities several times with 200 μl of PBS. The samples were centrifuged to remove insoluble debris and supernatant was immediately analyzed for specific antibodies. For collection of intestinal secretory antibodies, a fraction of the small intestine (approximately 3 cm long) was excised and cut perpendicularly to open the intestinal tubes. The excised samples were immersed in 0.5 ml of PBS and vigorously vortexed, followed by centrifugation to remove insoluble debris. Supernatant was used for antibody analysis.

Antibody titer determination by enzyme-linked immunosorbent assay (ELISA) for serum, nasal and intestinal secretions. Serum and mucosal samples were analyzed for the presence of specific antibodies by ELISA as described previously (1). Briefly, 96-well ELISA plates (Sumilon, Sumitomo Bakelite, Japan) were coated with recombinant Pfs25 proteins (33). The plates were washed with PBS containing 0.05% Tween-20 (PBST) three times and blocked with 1% BSA in PBS. Serial dilutions of serum samples were applied to wells in duplicates. Secondary antibodies specific for each mouse antibody isotype (immunoglobulin G [IgG], IgM and IgA) and IgG subclass (IgG1, IgG2a, IgG2b, and IgG3) was used for detection. Optical density (OD) was measured by microplate reader (Bio-Rad Laboratories) at 415 nm. The OD_{415} value of 0.1 was used as the baseline to determine the endpoint titers for specific serum IgG. In some experiments, serum antibody levels were expressed as OD_{415} measurement after making appropriate dilutions as indicated. Antibodies present in nasal secretions were analyzed by diluting the nasal washings by 15-fold with PBS before applying the samples to microtiter plates. To analyze specific antibodies in intestinal secretions, intestinal washings collected as described above were diluted with PBS by 2-fold prior to ELISA. Student's t test was performed to compare antibody levels of serum and mucosal samples between different test groups.

Recognition of native parasite by immunofluorescence assay. All human materials used in this study were reviewed and approved by the Institutional Ethics Committee of the Thai Ministry of Public Health and the Human Subjects Research Review Board of the United States Army. For purification of gametocytes, peripheral blood was collected by heparinized syringes under written informed consent from patients who came to the malaria clinics in the Mae Sod district in the Tak province of northwestern Thailand. Infection with *P. falciparum* was confirmed by Giemsa stain of thick and thin blood smears. Cultured *P. falciparum* parasite preparations rich in zygotes and small numbers of ookinetes were spotted on slides and fixed with acetone as previously described (25). The slides were blocked with PBS containing 5% nonfat milk and incubated with Pfs25/CT immune sera. The slides were washed with ice-cold PBS for 5 min and incubated with fluorescein isothiocyanate-conjugated anti-mouse antibody, followed by washing with ice-cold PBS. Slides were examined by confocal scanning laser microscope (Nikon C-1).

Transmission-blocking assays. Peripheral blood was collected from four volunteer patients as described above. Their parasitemia were ranging from 0.04 to 0.18%, and gametocytemia from 0.002% to 0.011%. Collected blood was aliquoted into tubes (300 μl/tube) and plasma was removed. Mouse immune sera were diluted (2-, 8- and 32-fold) with heat-inactivated normal human AB serum prepared from malaria naïve donors. Each diluted test serum was mixed with *P. falciparum*-infected blood cells as described above (1:1 vol/vol ratio) and incubated for 15 min at room temperature. The mixture was placed in a membrane feeding apparatus kept at 37°C to allow starved *Anopheles dirus* A mosquitoes (Bangkok colony, Armed Forces Research Institute of Medical Sciences) to feed on the blood meals for 30 min. Unfed mosquitoes were removed and only fully engorged mosquitoes were maintained for a week by giving 10% sucrose water in the insectary.

For each mouse test immune serum, 20 mosquitoes (i.e., a total of 80 mosquitoes for four patients' blood samples) were dissected and analyzed by staining with 0.5% mercurochrome to count the number of oocysts developed within the mosquito midgut under the microscope. Mann-Whitney U test was used to examine the difference in oocyst counts per mosquito between control and immunized groups. Fisher's exact probability test was used to examine the difference of infection rates between control and immunized groups. P values less than 0.05 were considered statistically significant.

RESULTS

Systemic and mucosal antibody responses induced in mice by intranasal immunizations. Immunization with Pfs25/CT resulted in a significant increment of specific anti-Pfs25 serum IgG responses ($P < 0.01$) (Fig. 1A). Higher IgG responses were induced in A/J than BALB/c mice, but the difference did not reach statistically significant level ($P = 0.23$). We also evaluated specific reactivity of immune sera against denatured forms of the recombinant Pfs25 proteins. We found that mucosally induced antibodies exhibited strict conformation-dependent reactivity, in which both A/J and BALB/c mouse immune sera recognized only native proteins, while no specific reaction was observed against denatured forms of the proteins ($P < 0.001$) (Fig. 1B). Mucosal immunization induced comparable levels of IgG1, IgG2a and IgG2b, but not IgG3 (Fig. 1C). Immunoglobulin isotypes other than IgG (i.e., IgM, IgE, and IgA) were also detected, although at relatively low levels in Pfs25/CT immune sera, but not in immune sera derived from intranasal administration of CT alone or PBS (Fig. 1D).

Next we analyzed mucosal antibody responses (Fig. 2). Intranasal immunization with Pfs25/CT induced significant levels of anti-Pfs25 IgA and IgG ($P < 0.01$) in nasal washings, whereas control mice given CT alone or PBS did not develop Pfs25-specific mucosal antibodies (Fig. 2A). IgG subclass analysis for nasal washings revealed a similar pattern seen for serum IgG subclasses (Fig. 2B). Mucosal adjuvant CT-specific IgA and IgG were also detected in nasal washings of mice immunized with Pfs25/CT or CT alone, but not in mice given PBS (Fig. 2C). Intranasal immunization also resulted in low but detectable levels of Pfs25-specific IgA and IgG in intestinal secretions of Pfs25/CT immunized group, but not in CT or PBS group, and the induced IgG subclass patterns were similar to that for nasal IgGs (data not shown).

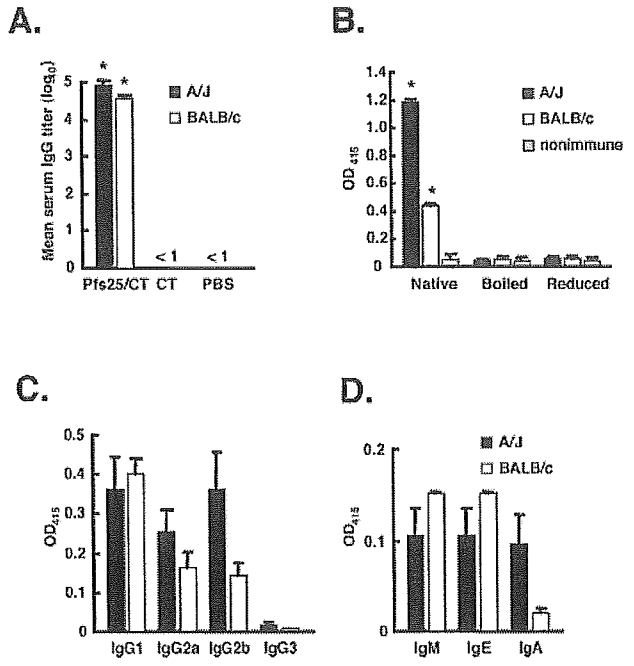

FIG. 1. Serum antibody responses induced by intranasal immunization of BALB/c and A/J mice with Pfs25/CT, CT alone, or PBS were analyzed by ELISA. Groups of six to seven mice were immunized three times at weeks 0, 3, and 5, and immune sera were collected at week 6 for analysis. A. Pfs25-specific serum IgG responses. Serum IgG titers were defined as the highest serum dilution giving 0.1 OD_{415}, and the data were expressed as the mean titers ± standard error. *, $P < 0.01$ versus CT alone or PBS. B. Conformation-dependent serum IgG responses. Data are expressed as the average OD_{415} ± standard error for immune sera diluted to 1:20,000. *, $P < 0.001$ versus boiled or reduced form of Pfs25 proteins. C. Serum IgG subclass analysis for Pfs25/CT immune sera. Data are expressed as the average OD_{415} ± standard error for immune sera diluted to 1:9,000. D. Analysis of serum Ig isotypes other than IgG (i.e., IgM, IgE, and IgA). Data were expressed as the average OD_{415} ± standard error for immune sera diluted to 1:3,000.

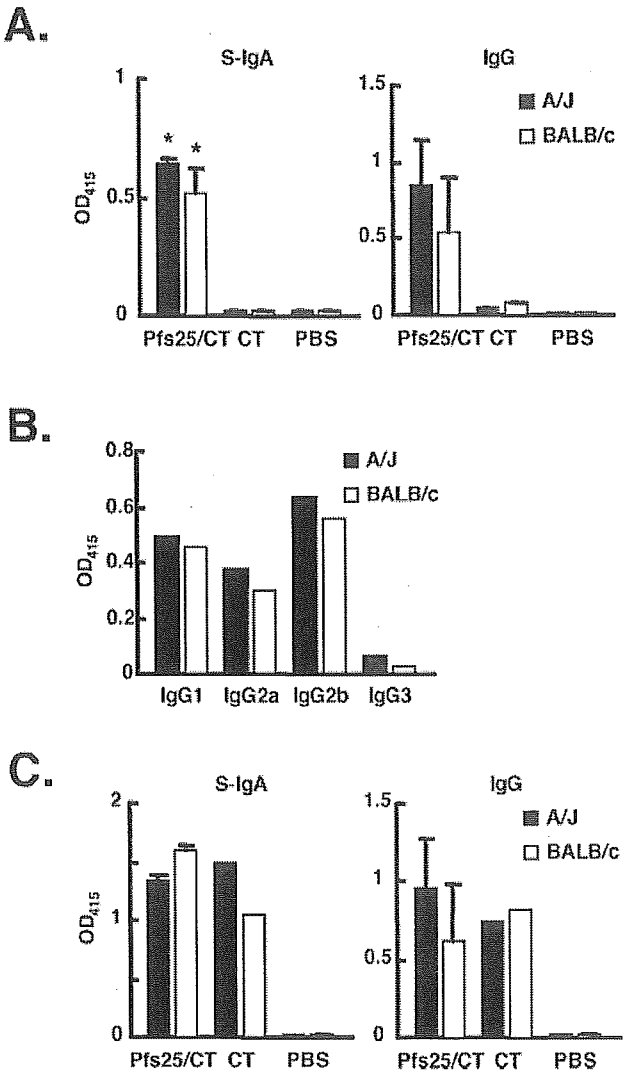

FIG. 2. Mucosal antibody responses induced by intranasal immunization of mice with Pfs25/CT, CT alone, or PBS were analyzed by ELISA. Nasal wash samples were collected immediately after exsanguination by washing the nasal cavities several times with 200 μl of PBS. The collected samples were diluted 15-fold with PBS prior to analysis. A. Pfs25-specific secretory IgA (S-IgA) and IgG in nasal secretions. Data are expressed as the average OD_{415} ± standard error. *, $P < 0.01$ versus CT alone or PBS. B. IgG subclass analysis of nasal IgG collected from mice immunized with Pfs25/CT. Results are expressed as the average OD_{415} of the pooled nasal washings. C. CT-specific secretory IgA and IgG in nasal secretions. Results are expressed as the average OD_{415} ± standard error.

Recognition of native Pfs25 proteins expressed at ookinete stage of *P. falciparum*. To evaluate antibody specificity of mucosally induced immune sera to native Pfs25 proteins, Pfs25/CT immune sera were reacted with cultured ookinete preparations. As indicated in Fig. 3, the immune sera specifically recognized ookinetes but not gametocytes. The fluorescent signal was localized on the surface of ookinetes, confirming that induced antibodies were capable of recognizing native Pfs25 proteins on the surface of ookinetes. The result was consistent with the expression patterns of the Pfs25 proteins in the parasites.

Evaluation of transmission-blocking activity. Transmission-blocking assays were performed using pooled immune sera of mice intranasally immunized with Pfs25/CT, CT alone or PBS. Pfs25/CT immune sera, but not control CT or PBS serum, had significant transmission-blocking activities, indicated by profound reduction of the numbers of oocysts developed in mosquito midgut (Table 1). Dilution of the immune sera resulted in reduction of transmission-blocking activities. In addition, Pfs25/CT immune sera significantly reduced mosquito infection rate defined as percent of infected mosquitoes in a total number of mosquitoes examined (Table 1). Serum dilution resulted in an increase in the infection rate.

We also analyzed the complete transmission-blocking rate, defined as the percentage of volunteers whose infected blood did not establish any parasite infection in mosquitoes (Table 1). All four human blood samples failed to transmit any parasite to mosquitoes when mixed with Pfs25/CT immune sera, but dilution of the immune sera gradually reduced the complete transmission-blocking rate.

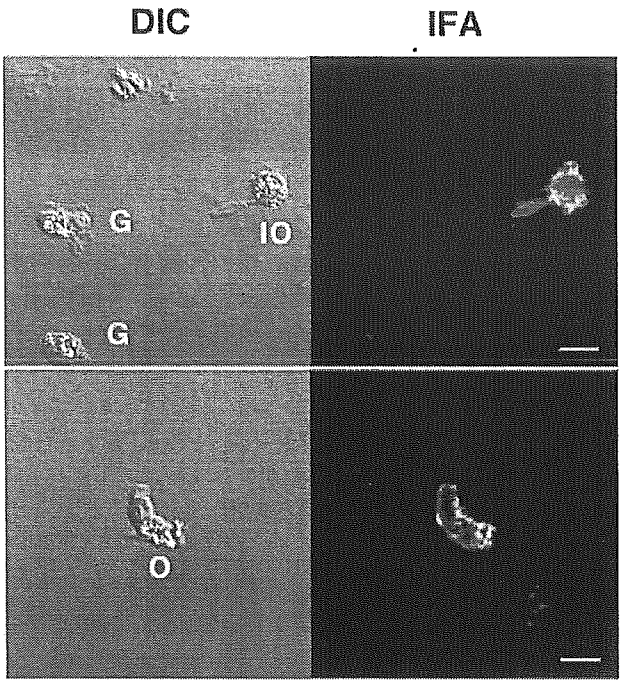

FIG. 3. Ookinete-specific reactivity of Pfs25/CT immune sera was confirmed by immunofluorescence analysis. The immune sera specifically recognized native Pfs25 proteins expressed on the surface of *P. falciparum* ookinetes. The immune sera did not react with gametocytes. DIC, differential interference contrast microscopy. IFA, fluorescence confocal scanning laser microscopy. G, gametocyte. IO, immature ookinete. O, mature ookinete. Bar = 5 μm.

We found strong correlations of Pfs25-specific serum antibody levels (Fig. 1) with the oocyst counts (correlation coefficient $r = -0.717$), with the mosquito infection rate ($r = -0.832$), and with the complete transmission-blocking rate ($r = 0.878$). In contrast, no correlation was observed between CT-specific antibody levels and the transmission-blocking activities.

DISCUSSION

With the prospect of developing noninvasive malaria transmission-blocking vaccines, we have previously demonstrated that intranasal immunization of recombinant Pvs25, an orthologous gene product of Pfs25 and a vaccine candidate against *P. vivax* malaria, induced a robust systemic immune response, conferring a significant protection against parasite transmission to mosquitoes (1). In this study we demonstrated a potent mucosal immunogenicity and protective efficacy of recombinant Pfs25 proteins (33). In addition, this is the first report indicating that a *P. falciparum* transmission-blocking vaccine candidate is effective against field-isolated parasites in a malaria-endemic area.

Our recent studies with rodent malaria *P. yoelii* also demonstrated that intranasal immunization of mice with recombinant Pys25 proteins (25) provided complete transmission-blocking immunity in both active and passive immunization regimens (unpublished data). Unlike the results of our previous studies with *P. vivax* (1) and *P. yoelii* (unpublished data), we found that the serum IgG subclasses induced by Pfs25/CT immunization were not strongly biased towards IgG1. It rather induced comparable levels of IgG1, IgG2a, and IgG2b (Fig. 1C), implying that mixed Th1 and Th2 responses were induced. Malkin et al. observed that the presence of heat-labile components in the membrane feeder enhanced the transmission-blocking activity of Pvs25 antisera (21). Because all heat-labile components were inactivated by heat treatment during the transmission-blocking assays performed in our present and previous studies, we might have underestimated the levels of actual transmission-blocking activity of mucosally induced immune sera. However, regardless of the types of immunity induced, specific antibody titers were the best correlate for protection, and no such correlation was found between CT-specific antibody titers and protective efficacy: these observations were consistent with other transmission-blocking vaccine studies (2, 7, 10, 11, 16, 18–20). Taken together, transmission-blocking activity was clearly correlated with levels of vaccine antigen-specific serum IgG, regardless of the reper-

TABLE 1. Transmission-blocking efficacy against Thai *Plasmodium falciparum* isolates

Mouse strain	Immunization	Serum dilution[a]	Median no. of oocysts with quartiles and ranges					P^b		Infection rate (%)[c]	P^d		Complete blocking rate (%)[e]
			Min	Lower	Median	Upper	Max	Vs. PBS	Vs. CT		Vs. PBS	Vs. CT	
A/J	PBS	1:2	0	0	0	9.0	108		0.0615	35/80 (43.8)		0.0505	0/4 (0)
	CT	1:2	0	0	0	3.8	68	0.0615		24/80 (30.0)	0.0505		0/4 (0)
	Pfs25/CT	1:2	0	0	0	0	0	<0.0001	<0.0001	0/80 (0)	<0.0001	<0.0001	4/4 (100)
		1:8	0	0	0	0	0	<0.0001	<0.0001	0/80 (0)	<0.0001	<0.0001	4/4 (100)
		1:32	0	0	0	0	10	0.0001	0.0529	17/80 (21.3)	0.0019	0.1386	0/4 (0)
BALB/c	PBS	1:2	0	0	4.5	28.5	130		0.3348	46/80 (57.5)		0.3752	1/4 (25)
	CT	1:2	0	0	2.0	19.5	109	0.3348		43/80 (53.8)	0.3752		0/4 (0)
	Pfs25/CT	1:2	0	0	0	0	0	<0.0001	<0.0001	0/80 (0)	<0.0001	<0.0001	4/4 (100)
		1:8	0	0	0	0	12	<0.0001	<0.0001	6/80 (7.5)	<0.0001	<0.0001	2/4 (50)
		1:32	0	0	0	0	12	<0.0001	<0.0001	19/80 (23.8)	0.0001	0.0001	1/4 (25)

[a] Dilution of test immune sera used for transmission-blocking assays.
[b] Determined by the Mann-Whitney *U* test for comparison of oocyst numbers between the test immune sera and PBS and CT sera.
[c] Number of infected mosquitoes/total number of mosquitoes examined.
[d] Determined by Fisher's exact probability test for comparison of mosquito infection rate between the test immune sera and PBS or CT sera.
[e] Number of patients whose blood samples did not result in any oocyst development in any mosquito examined/total number of volunteer patients ($n = 4$).

toire of IgG subclasses induced, strain of mouse used, difference in *Plasmodium* species targeted, or type of immunization method employed.

In contrast to the general perception that mucosal vaccines are much less effective for the induction of systemic antibody responses than parenteral vaccines, we found that intranasal vaccines, when coadministered with a strong mucosal adjuvant like CT, are not necessarily considered inferior to parenteral vaccines at least in a murine model (1, 2, 16, 18; unpublished data). Systemic antibodies raised against *Pichia pastoris*-expressed recombinant Pfs25 proteins (33) by intranasal immunization specifically recognized native proteins expressed on ookinete surface (Fig. 3), but barely recognized heat-denatured or reduced form of proteins (Fig. 1B), indicating that at least some conformational epitopes were retained in the course of intranasal immunization and correctly presented to the immune system in an intact form for the induction of biologically active antibodies that functioned as transmission-blocking agents within the mosquito midgut.

The highly efficacious transmission-blocking activity observed with mucosally induced immune sera supports the potential of applying mucosal vaccines to malaria prophylactics. Further, our recent mucosal immunization studies with various antigens such as formalin-inactivated Japanese encephalitis virus vaccine and the paramyosin antigen of *Schistosoma japonicum* demonstrated that mucosal vaccines induced strong and long-lasting humoral as well as cellular immunity comparable to that with parenteral vaccines when strong adjuvants like CT were coadministered (unpublished data). These results indicate that CT is a strong immune potentiator that may be able to induce immunological memory against heterologous antigens in a rodent model. However, CT needs to be precluded from clinical use due to its enterotoxicity and potential hazardous effects on olfactory nerves (12). Therefore, the particular vaccination regimen presented in this study using CT as an adjuvant needs to be considered as a model system to prove the effectiveness of mucosal vaccines against malaria transmission.

Since the mucosal immunogenicity of Pfs25 may not depend on a particular mucosal adjuvant or delivery system, specific targeting or immunomodulation of professional antigen-presenting cells such as dendritic cells and B cells with other, potentially safer agents (3, 8, 9, 22, 26, 28, 31) than CT may offer new approaches for the development of malaria vaccines and warrant further evaluation of mucosal and other less invasive vaccination regimens as alternative strategies for malaria control in the future.

ACKNOWLEDGMENTS

This work was supported in part by Grants-in-Aid for Scientific Research 16390125, 16406009, and 14770111 and Grant-in-Aid for Scientific Research on Priority Areas 16017273 from the Ministry of Education, Culture, Sports, Science and Technology, and a Grant for International Health Cooperation Research (15C-5) from the Ministry of Health, Labor and Welfare, Japan. This work also received financial support from the Bio-oriented Technology Research Advancement Institution (BRAIN), Japan.

We thank Jeeraphat Sirichaisinthop and the staffs of the Office of Vector-Borne Disease Control 1, Saraburi, Thailand, for constant help in setting up the field sites, and the staffs of the Department of Entomology, AFRIMS, Bangkok, Thailand. We also thank the Malaria Vaccine Initiative at the Program for Appropriate Technology in Health for their constant help with transmission-blocking vaccine development.

REFERENCES

1. **Arakawa, T., T. Tsuboi, A. Kishimoto, J. Sattabongkot, N. Suwanabun, T. Rungruang, Y. Matsumoto, N. Tsuji, H. Hisaeda, A. Stowers, I. Shimabukuro, Y. Sato, and M. Torii.** 2003. Serum antibodies induced by intranasal immunization of mice with *Plasmodium vivax* Pvs25 co-administered with cholera toxin completely block parasite transmission to mosquitoes. Vaccine **21**:3143–3148.
2. **Barr, P. J., K. M. Green, H. L. Gibson, I. C. Bathurst, I. A. Quakyi, and D. C. Kaslow.** 1991. Recombinant Pfs25 protein of *Plasmodium falciparum* elicits malaria transmission-blocking immunity in experimental animals. J. Exp. Med. **174**:1203–1208.
3. **Boyle, J. S., J. L. Brady, and A. M. Lew.** 1998. Enhanced responses to a DNA vaccine encoding a fusion antigen that is directed to sites of immune induction. Nature **392**:408–411.
4. **Breman, J. G., M. S. Alilio, and A. Mills.** 2004. Conquering the intolerable burden of malaria: what's new, what's needed: a summary. Am. J. Trop. Med. Hyg. **71**(2 Suppl.):1–15.
5. **Carcaboso, A. M., R. M. Hernandez, M. Igartua, J. E. Rosas, M. E. Patarroyo, and J. L. Pedraz.** 2004. Potent, long lasting systemic antibody levels and mixed Th1/Th2 immune response after nasal immunization with malaria antigen loaded PLGA microparticles. Vaccine **22**:1423–1432.
6. **Carter, R.** 2001. Transmission blocking malaria vaccines. Vaccine **19**:2309–2314.
7. **Coban, C., M. T. Philipp, J. E. Purcell, D. B. Keister, M. Okulate, D. S. Martin, and N. Kumar.** 2004. Induction of *Plasmodium falciparum* transmission-blocking antibodies in nonhuman primates by a combination of DNA and protein immunizations. Infect. Immun. **72**:253–259.
8. **Eriksson, A., and N. Lycke.** 2003. The CTA1-DD vaccine adjuvant binds to human B cells and potentiates their T cell stimulating ability. Vaccine **22**: 185–193.
9. **Eriksson, A. M., K. M. Schon, and N. Y. Lycke.** 2004. The cholera toxin-derived CTA1-DD vaccine adjuvant administered intranasally does not cause inflammation or accumulate in the nervous tissues. J. Immunol. **173**: 3310–3319.
10. **Gozar, M. M., O. Muratova, D. B. Keister, C. R. Kensil, V. L. Price, and D. C. Kaslow.** 2001. *Plasmodium falciparum*: immunogenicity of alum-adsorbed clinical-grade TBV25-28, a yeast-secreted malaria transmission-blocking vaccine candidate. Exp. Parasitol. **97**:61–69.
11. **Gozar, M. M., V. L. Price, and D. C. Kaslow.** 1998. *Saccharomyces cerevisiae*-secreted fusion proteins Pfs25 and Pfs28 elicit potent *Plasmodium falciparum* transmission-blocking antibodies in mice. Infect. Immun. **66**:59–64.
12. **Hagiwara, Y., T. Iwasaki, H. Asanuma, Y. Sato, T. Sata, C. Aizawa, T. Kurata, and S. Tamura.** 2001. Effects of intranasal administration of cholera toxin (or *Escherichia coli* heat-labile enterotoxin) B subunits supplemented with a trace amount of the holotoxin on the brain. Vaccine **19**:1652–1660.
13. **Haneberg, B., and J. Holst.** 2002. Can. nonliving nasal vaccines be made to work? Expert Rev. Vaccines **1**:227–232.
14. **Harandi, A. M., J. Sanchez, K. Eriksson, and J. Holmgren.** 2003. Recent developments in mucosal immunomodulatory adjuvants. Curr. Opin. Investig. Drugs **4**:156–161.
15. **Hirunpetcharat, C., D. Stanisic, X. Q. Liu, J. Vadolas, R. A. Strugnell, R. Lee, L. H. Miller, D. C. Kaslow, and M. F. Good.** 1998. Intranasal immunization with yeast-expressed 19 kD carboxyl-terminal fragment of *Plasmodium yoelii* merozoite surface protein-1 (yMSP119) induces protective immunity to blood stage malaria infection in mice. Parasite Immunol. **20**: 413–420.
16. **Hisaeda, H., A. W. Stowers, T. Tsuboi, W. E. Collins, J. S. Sattabongkot, N. Suwanabun, M. Torii, and D. C. Kaslow.** 2000. Antibodies to malaria vaccine candidates Pvs25 and Pvs28 completely block the ability of *Plasmodium vivax* to infect mosquitoes. Infect. Immun. **68**:6618–6623.
17. **Kaslow, D. C., I. A. Quakyi, C. Syin, M. G. Raum, D. B. Keister, J. E. Coligan, T. F. McCutchan, and L. H. Miller.** 1988. A vaccine candidate from the sexual stage of human malaria that contains EGF-like domains. Nature **333**:74–76.
18. **Kaslow, D. C., I. C. Bathurst, T. Lensen, T. Ponnudurai, P. J. Barr, and D. B. Keister.** 1994. *Saccharomyces cerevisiae* recombinant Pfs25 adsorbed to alum elicits antibodies that block transmission of *Plasmodium falciparum*. Infect. Immun. **62**:5576–5580.
19. **Kongkasuriyachai, D., L. Bartels-Andrews, A. Stowers, W. E. Collins, J. Sullivan, J. Sattabongkot, M. Torii, T. Tsuboi, and N. Kumar.** 2004. Potent immunogenicity of DNA vaccines encoding *Plasmodium vivax* transmission-blocking vaccine candidates Pvs25 and Pvs28-evaluation of homologous and heterologous antigen-delivery prime-boost strategy. Vaccine **22**:3205–3213.
20. **Lobo, C. A., R. Dhar, and N. Kumar.** 1999. Immunization of mice with DNA-based Pfs25 elicits potent malaria transmission-blocking antibodies. Infect. Immun. **67**:1688–1693.
21. **Malkin, E. M., A. P. Durbin, D. J. Diemert, J. Sattabongkot, Y. Wu, K. Miura, C. A. Long, L. Lambert, A. P. Miles, J. Wang, A. Stowers, L. H.**

Miller, and A. Saul. 2005. Phase 1 vaccine trial of Pvs25H: a transmission blocking vaccine for *Plasmodium vivax* malaria. Vaccine **23**:3131–3138.
22. **Niikura, M., S. Takamura, G. Kim, S. Kawai, M. Saijo, S. Morikawa, I. Kurane, T. C. Li, N. Takeda, and Y. Yasutomi.** 2002. Chimeric recombinant hepatitis E virus-like particles as an oral vaccine vehicle presenting foreign epitopes. Virology **293**:273–280.
23. **Schorr, J., B. Knapp, E. Hundt, H. A. Kupper, and E. Amann.** 1991. Surface expression of malarial antigens in *Salmonella typhimurium*: induction of serum antibody response upon oral vaccination of mice. Vaccine **9**:675–681.
24. **Somner, E. A., S. A. Ogun, K. A. Sinha, L. M. Spencer Valero, J. J. Lee, J. A. Harrison, A. A. Holder, C. E. Hormaeche, and C. M. Khan.** 1999. Expression of disulphide-bridge-dependent conformational epitopes and immunogenicity of the carboxy-terminal 19 kDa domain of *Plasmodium yoelii* merozoite surface protein-1 in live attenuated *Salmonella* vaccine strains. Microbiology **145**:221–229.
25. **Tsuboi, T., Y. M. Cao, Y. Hitsumoto, T. Yanagi, H. Kanbara, and M. Torii.** 1997. Two antigens on zygotes and ookinetes of *Plasmodium yoelii* and *Plasmodium berghei* that are distinct targets of transmission-blocking immunity. Infect. Immun. **65**:2260–2264.
26. **van der Lubben, I. M., G. Kersten, M. M. Fretz, C. Beuvery, J. Coos Verhoef, and H. E. Junginger.** 2003. Chitosan microparticles for mucosal vaccination against diphtheria: oral and nasal efficacy studies in mice. Vaccine **21**:1400–1408.
27. **Wang, L., L. Kedzierski, S. L. Wesselingh, and R. L. Coppel.** 2003. Oral immunization with a recombinant malaria protein induces conformational antibodies and protects mice against lethal malaria. Infect. Immun. **71**:2356–2364.
28. **Watanabe, I., T. M. Ross, S. Tamura, T. Ichinohe, S. Ito, H. Takahashi, H. Sawa, J. Chiba, T. Kurata, T. Sata, and H. Hasegawa.** 2003. Protection against influenza virus infection by intranasal administration of C3d-fused hemagglutinin. Vaccine **21**:4532–4538.
29. **World Health Organization.** 2002. Annex table 3: burden of disease in DALYs by cause, sex and mortality stratum in W.H.O. regions, estimates for 2001. World Health Report, 2002: reducing risks, promoting healthy life, 192–197. World Health Organization, Geneva, Switzerland.
30. **Wu, S., M. Beier, M. B. Sztein, J. Galen, T. Pickett, A. A. Holder, O. G. Gomez-Duarte, and M. M. Levine.** 2000. Construction and immunogenicity in mice of attenuated *Salmonella typhi* expressing *Plasmodium falciparum* merozoite surface protein 1 (MSP-1) fused to tetanus toxin fragment C. J. Biotechnol. **83**:125–135.
31. **Wu, Y., X. Wang, K. L. Csencsits, A. Haddad, N. Walters, and D. W. Pascual.** 2001. M cell-targeted DNA vaccination. Proc. Natl. Acad. Sci. USA **98**:9318–9323.
32. **Yuki, Y., and H. Kiyono.** 2003. New generation of mucosal adjuvants for the induction of protective immunity. Rev. Med. Virol. **13**:293–310.
33. **Zou, L., A. P. Miles, J. Wang, and A. W. Stowers.** 2003. Expression of malaria transmission-blocking vaccine antigen Pfs25 in *Pichia pastoris* for use in human clinical trials. Vaccine **21**:1650–1657.

Editor: W. A. Petri, Jr.

Available online at www.sciencedirect.com
SCIENCE DIRECT®
The International Journal of Biochemistry & Cell Biology 37 (2005) 700–706
IJBCB
www.elsevier.com/locate/biocel

Medicine in focus

Malaria: immune evasion by parasites

Hajime Hisaeda[a,*], Koji Yasutomo[b], Kunisuke Himeno[a]

[a] *Department of Parasitology, Graduate School of Medical Sciences, Kyushu University, 3-1-1 Maidashi, Higashi-ku Fukuoka 812-8582, Japan*
[b] *Department of Immunology and Parasitology, Institute of Health Biosciences, The University of Tokushima Graduate School, 3-18-15 Kuramoto, Tokushima 770-8503, Japan*

Received 21 June 2004; received in revised form 7 October 2004; accepted 13 October 2004

Abstract

Malaria is one of the most life-threatening infectious diseases worldwide. Specific immunity to natural infection is acquired slowly despite a high degree of repeated exposure and rarely continues for a long time even in endemic areas. Malaria parasites have evolved to acquire diverse immune evasion mechanisms that evoke poor immune responses and allow infection of individuals previously exposed. The shrewd schema of malaria parasites also hampers the development of effective vaccines. Furthermore, some of those mechanisms are essential for malaria pathogenesis. In this article, an outline of protective immunity to malaria is given, then strategies used by malaria parasites to evade host immunity, including antigen diversity/polymorphism, antigen variation and total immune suppression, are reviewed. Finally, trials to control malaria based on accumulating insights into the host–parasite relationship are discussed.

Keywords: Malaria; Immune evasion; Regulatory T cells

1. Introduction

Malaria is an arthropod-borne disease caused by infection with the protozoan parasite genus *Plasmodium*, of which four species infect humans. Each year, there are 200–300 million episodes of acute malaria illness and 2.5 million people die from the disease. *Plasmodium falciparum* causes the most malignant disease, responsible for nine of 10 deaths from malaria, mostly in children in sub-Saharan Africa. In patients with *falciparum* malaria, parasite growth sometimes is not controlled, and these patients can suffer from cerebral malaria or other fatal complications of malignant malaria, as the infection progresses. Antibodies and T cells play crucial roles in protective immunity against malaria parasites. However, it is difficult to acquire long-lasting immunity, despite frequent exposure to parasites in endemic regions. There are many reasons for the low immunogenicity of malaria parasites. We

* Corresponding author. Tel.: +81 92 642 6119; fax: +81 92 642 6115.
E-mail address: hisa@parasite.med.kyushu-u.ac.jp (H. Hisaeda).

1357-2725/$ – see front matter © 2004 Elsevier Ltd. All rights reserved.
doi:10.1016/j.biocel.2004.10.009